JAERI-Research
97-081

INVESTIGATION ON THE EVALUATION OF CLEAVAGE FRACTURE TOUGHNESS USING PCCv SPECIMENS IN THE DUCTILE-BRITTLE TRANSITION RANGE OF REACTOR PRESSURE VESSEL STEELS (CONTRACT RESEARCH)

November 1997

Kunio ONIZAWA, Tohru TOBITA and Masahide SUZUKI

日本原子力研究所
Japan Atomic Energy Research Institute

本レポートは，日本原子力研究所が不定期に公刊している研究報告書です。
入手の問合わせは，日本原子力研究所研究情報部研究情報課（〒319-11 茨城県那珂郡東海村）あて，お申し越しください。なお，このほかに財団法人原子力弘済会資料センター（〒319-11 茨城県那珂郡東海村日本原子力研究所内）で複写による実費頒布をおこなっております。

This report is issued irregularly.
Inquiries about availability of the reports should be addressed to Research Information Division, Department of Intellectual Resources, Japan Atomic Energy Research Institute, Tokai-mura, Naka-gun, Ibaraki-ken 319-11, Japan.

編集兼発行　日本原子力研究所
印　　刷　㈱原子力資料サービス

Investigation on the Evaluation of Cleavage Fracture Toughness Using PCCv Specimens in the Ductile-brittle Transition Range of Reactor Pressure Vessel Steels
(Contract Research)

Kunio ONIZAWA, Tohru TOBITA and Masahide SUZUKI

Department of Reactor Safety Research
Nuclear Safety Research Center
Tokai Research Establishment
Japan Atomic Energy Research Institute
Tokai-mura, Naka-gun, Ibaraki-ken

(Received Octorber 3, 1997)

To obtain a reliable fracture toughness value for the cleavage fracture initiation in the ductile-brittle transition range of RPV steels, the applicability of precracked Charpy-v (PCCv) specimens was investigated. An approach based on the weakest link theory and fractographic observation were applied to analyze the specimen size effect and the scatter of fracture toughness values. The materials used were four kinds of ASTM A533B class 1 steels that were all manufactured by Japanese steel makers.

The specimen size effect on cleavage fracture toughness was seen between PCCv and 1T-CT specimens. To obtain the equivalent data from PCCv specimens to 1T-CT specimens, the size correction scheme based on the weakest link theory was applied to the PCCv data. However, it was found that the size effect was still remained to some extent. The fracture toughness transition curve was evaluated by means of the master curve approach which was

This report includes the test results carried out under the contract between JAERI and Science and Technology Agency of Japan under the auspices of the special account law for electric power development promotion.

being proposed by the ASTM. The master curve determined by PCCv data tended to overestimate the fracture toughness at the upper transition range where PCCv data would be invalid. According to the master curve approach using valid PCCv data sets, it was shown that the shift of the master curve by irradiation was somewhat greater than the Charpy 41J shift.

Through fractographic observation, the ductile crack growth before a cleavage fracture was characterized and the initiation site of cleavage fracture was determined.

Keywords: Pressure Vessel Steel, Fracture Toughness, Transition, Brittle Fracture, Statistical Analysis, Size Effect, Lower Bound, Irradiation Embrittlement, Transition Temperature Shift

予き裂シャルピー試験片による圧力容器鋼材の延性脆性遷移温度域における へき開破壊靱性の評価に関する検討 （受託研究）

日本原子力研究所東海研究所安全性試験研究センター原子炉安全工学部
鬼沢　邦雄・飛田　　徹・鈴木　雅秀

（1997年10月3日受理）

原子炉圧力容器用鋼材の延性脆性遷移温度域におけるへき開破壊開始時の破壊靱性値を精度良く求めるため、予き裂付きシャルピー型破壊靭性（PCCv）試験片の適用性を検討した。PCCv試験片から得られる破壊靭性値の寸法効果とばらつきを分析するため、最弱リンク理論に基づく手法と破面観察を実施した。使用した鋼材は、4種類の国産圧力容器用ASTM A533Bクラス1鋼である。

PCCvと1T-CT試験片から得られる破壊靭性値には、試験片寸法効果が認められた。PCCv試験片から1T-CTと同等の破壊靭性を得るために、最弱リンク理論に基づく試験片寸法効果の補正式をPCCvデータに適用した。しかしながら、寸法効果は十分には補正しきれずにある程度残ることがわかった。また、破壊靭性の温度依存性、すなわち、破壊靭性遷移曲線を求めるため、ASTMで提案されているマスターカーブ法を適用した。PCCv試験片から求めた破壊靭性遷移曲線は、PCCvデータが有効でない上部遷移温度域では過大評価となる傾向を示した。PCCv試験片の有効なデータから求めたマスターカーブを利用して、破壊靭性遷移曲線の照射によるシフトを求めると、シャルピー41Jレベルの遷移温度シフトより大きいことが示された。

試験片の破面観察により、へき開破壊前の延性き裂成長を特徴付けるとともに、破面上のへき開破壊の開始位置についての情報を取得した。

本報告書は、電源開発促進対策特別会計法に基づき、科学技術庁からの委託によって行った研究の成果を含む。

東海研究所：〒319-11　茨城県那珂郡東海村白方白根2-4

Contents

目　　次

1. INTRODUCTION

Ferritic steel shows a ductile-to-brittle transition in fracture behavior at a relatively low temperature. Since a reactor pressure vessel (RPV) is made from the ferritic steel, it may be fractured in a brittle manner at lower temperature than the transition when a certain crack exists in the vessel. The brittle fracture of an RPV must be prevented, because it may lead to a catastrophic fracture of the vessel followed by severe accident. Therefore, the RPV is operated at higher temperature than the ductile-to-brittle transition temperature. However, fast neutrons from the reactor core during operation can cause the increase of the transition temperature, i.e., the irradiation embrittlement of the vessel material. To assure the structural integrity of an RPV throughout the operational life, the fracture toughness values after neutron irradiation are needed. To do this, the design codes for the RPV require surveillance specimens such as Charpy impact specimens be installed in the RPV to evaluate the degree of irradiation embrittlement. Charpy impact tests in the surveillance tests is implemented mainly to evaluate the embrittlement of RPV steels in terms of the shift of the transition temperature. Then the results obtained from the surveillance tests according to the codes are used with empirical correlation between Charpy impact properties and fracture toughness values.[1, 2] Most of the codes assume that the degree of irradiation embrittlement obtained from Charpy impact tests are identical to that of fracture toughness for the material concerned. Recent research, however, has indicated that the correlation is not always conservative in predicting the degree of irradiation embrittlement in terms of fracture toughness.[3,4] Fracture mechanics methodology is, therefore, necessary for the precise evaluation of irradiation embrittlement to assure the structural integrity of an RPV.

Regarding the issue mentioned above, a methodology to evaluate fracture toughness of RPV steels has not been established completely, particularly in the transition range. As the fracture toughness values of the RPV steel show a large scatter in the ductile-to-brittle transition range, the fracture toughness can not be evaluated without some levels of uncertainty. This means that a certain statistical approach is necessary for the evaluation of the fracture toughness. Fracture toughness values from small size specimens, such as surveillance specimens, also show large effects on specimen size. Although intensive research[e.g. 5] has been conducted to establish the statistical treatment and the evaluation method of size effects in the past, the methods need a large number of specimens and/or relatively large size specimens.[6] The number and the size of surveillance specimens are limited by the small volume of a surveillance capsule. Therefore, further research is desired to resolve the limitation and to establish an improved surveillance test method that is applicable for the small number and the small sizes of specimens.

This paper describes the results of fracture toughness tests using four kinds of pressure vessel steels including an IAEA reference material JRQ. Based on the results of the fracture toughness tests using precracked Charpy specimens and standard size 1T-CT specimens, a statistical analysis and a fractographic study were performed to evaluate the lower bound toughness within the transition temperature range. An effect of specimen size on fracture toughness value is investigated by using the equation proposed by Wallin[7] based on the weakest

link theory.[8] The data scatter of the experimental data is also compared with the theory. The master curve approach which was proposed by Wallin[9] and the ASTM[10] is applied to estimate the temperature dependence of cleavage fracture toughness. The results of post irradiation tests for JRQ are also presented and compared with the results from the corresponding Charpy impact tests. Fractographic observation is also performed to characterize the ductile crack growth before cleavage fracture and the initiation site of cleavage fracture. A part of this report was performed at JAERI in the framework of the IAEA Coordinated Research Program Phase-3[11].

2. EXPERIMENTS

2.1 Materials

Materials used in this study were four kinds of pressure vessel steels of ASTM A533B class 1. The one is designated JRQ, which was used as a correlation monitor material in the IAEA CRP-3[12]. The another material was chosen to have a large number of database for cleavage fracture toughness from small size specimens to large ones. The material is designated as JSPS A533B-1 which was used in the round robin study organized by The Japan Society for Promoting of Science (JSPS)[13]. The other materials were made as A533B-1 steels which were called as Steel A and Steel B that corresponded to the old age RPV steel and the modern steel, respectively. Chemical compositions of the materials are summarized in Table 1. Mechanical properties at room temperature for the materials used are listed in Table 2.

2.2 Fracture Toughness Tests

We used four types of specimens, precracked Charpy (PCCv), 0.5T-DCT, 1T-CT and 4T-CT. In some cases the specimens were side-grooved by 10% on each side of the specimen after precracking. For JSPS A533B-1 steel, one of the authors performed fracture toughness tests using PCCv specimens machined from halves of broken 2T-CT specimens at SCK/CEN.[14] The notch orientation of the specimens is T-L direction for all specimens. All specimens were machined from the approximately quarter thickness position of the material. Fracture toughness tests were performed at mainly lower transition temperature range which a cleavage fracture was occurred before the limit load of the specimen. Some specimens were tested at an upper shelf temperature range to obtain J-R curves.

Testing and evaluation for fracture toughness were performed according to ASTM standards[15,16] and JSME method[17]. As a valid plane-strain fracture toughness, K_{IC}, could not be obtained by the specimens tested except for a few 4T-CT specimens of Steels A and B, the following method was applied to obtain elastic-plastic fracture toughness. Fracture toughness values at cleavage fracture, Jc, were calculated based on the area under load-displacement curve up to the sudden load drop and the cleavage fracture load (see eq. 1). Fracture toughness K_{JC} values were then converted from J_C by the following equation (2). Elastic modulus E and

link theory.[8] The data scatter of the experimental data is also compared with the theory. The master curve approach which was proposed by Wallin[9] and the ASTM[10] is applied to estimate the temperature dependence of cleavage fracture toughness. The results of post irradiation tests for JRQ are also presented and compared with the results from the corresponding Charpy impact tests. Fractographic observation is also performed to characterize the ductile crack growth before cleavage fracture and the initiation site of cleavage fracture. A part of this report was performed at JAERI in the framework of the IAEA Coordinated Research Program Phase-3[11].

2. EXPERIMENTS

2.1 Materials

Materials used in this study were four kinds of pressure vessel steels of ASTM A533B class 1. The one is designated JRQ, which was used as a correlation monitor material in the IAEA CRP-3[12]. The another material was chosen to have a large number of database for cleavage fracture toughness from small size specimens to large ones. The material is designated as JSPS A533B-1 which was used in the round robin study organized by The Japan Society for Promoting of Science (JSPS)[13]. The other materials were made as A533B-1 steels which were called as Steel A and Steel B that corresponded to the old age RPV steel and the modern steel, respectively. Chemical compositions of the materials are summarized in Table 1. Mechanical properties at room temperature for the materials used are listed in Table 2.

2.2 Fracture Toughness Tests

We used four types of specimens, precracked Charpy (PCCv), 0.5T-DCT, 1T-CT and 4T-CT. In some cases the specimens were side-grooved by 10% on each side of the specimen after precracking. For JSPS A533B-1 steel, one of the authors performed fracture toughness tests using PCCv specimens machined from halves of broken 2T-CT specimens at SCK/CEN.[14] The notch orientation of the specimens is T-L direction for all specimens. All specimens were machined from the approximately quarter thickness position of the material. Fracture toughness tests were performed at mainly lower transition temperature range which a cleavage fracture was occurred before the limit load of the specimen. Some specimens were tested at an upper shelf temperature range to obtain J-R curves.

Testing and evaluation for fracture toughness were performed according to ASTM standards[15,16] and JSME method[17]. As a valid plane-strain fracture toughness, K_{IC}, could not be obtained by the specimens tested except for a few 4T-CT specimens of Steels A and B, the following method was applied to obtain elastic-plastic fracture toughness. Fracture toughness values at cleavage fracture, Jc, were calculated based on the area under load-displacement curve up to the sudden load drop and the cleavage fracture load (see eq. 1). Fracture toughness K_{JC} values were then converted from J_C by the following equation (2). Elastic modulus E and

Poisson's ratio ν were fixed to 206 GPa and 0.3 in this study, respectively.

$$J_C = J_{el} + J_{pl} = \frac{K_C^{\,2}}{E'} + \frac{\eta A_{pl}}{B_N b_0} \quad (1)$$

where Kc: Stress intensity factor at the cleavage fracture,

η=2+0.522*(a_0/W) for compact specimens,

η=2 for PCCv specimens,

A_{pl}: Plastic part of the area under load-displacement curve,

B_N: Net thickness, b_0: Initial ligament (=W-a_0),

A_0: Initial crack length, W: Specimen width,

E'=E for ASTM, E'=E/(1-ν^2) for JSME.

$$K_{JC} = \sqrt{E' J_C} \quad (2)$$

In the ASTM draft method, η factor has been changed from 2.0 to 1.9 based on the 3-D detailed analysis for PCCv specimen.[18] This makes the fracture toughness value lower by maximum 5% in terms of J-integral. When some equations in the ASTM draft method are applied to the data, the new η factor was used.

At upper shelf temperature range, J_{IC} values and J-R curves for the materials except for the JSPS A533B-1 were obtained based on the JSME method. Ductile crack growth in a specimen during a test was measured by unloading elastic compliance method. The major difference in both methods is the range of valid data to determine a J_{IC_JSME} value. The ASTM method utilizes the data between a 0.15 mm offset line and a 1.5 mm offset line, while the JSME method uses the data up to ductile crack extension of 1.0 mm. In addition, the JSME method recommends a blunting line for A533B-1 steel as follows:

$$J = 4\sigma_Y \bullet \Delta a \quad (3)$$

This equation for a blunting line has been established based on the results from a fractographic observation of stretch zone width.[16] A J_{IC_JSME} value is defined by the intersection of the blunting line and J-R curve. The J_{IC_JSME} value is then considered as an actual initiation of ductile crack growth. Therefore, this equation was applied in this study to investigate a ductile crack extension before cleavage fracture in the transition region.

2.3 Irradiation

Specimens of JRQ were irradiated in Japan Materials Testing Reactor (JMTR, thermal output 50MW). Two types of fracture toughness specimens, PCCv and 0.5T-DCT were irradiated. Fast neutron fluence for the specimens was 1.9~2.5 x 10^{19} n/cm^2 (E>1 MeV). The displacement per atom (dpa) for iron by the irradiation to 2 x 10^{19} n/cm^2 (E>1 MeV) was about 3 x 10^{-2}. Fast neutron flux was about 1.2 x 10^{13} n/cm^{2}s (E>1 MeV). Temperature for the specimens during irradiation was controlled in the range from 280 to 300 ℃. The shifts of Charpy transition temperatures and the hardening by neutron irradiation are summarized in Table 3[11].

Specimens of Steel A and Steel B are also being irradiated at JMTR. Sixteen PCCv

specimens of the steels were encapsuled with ten Charpy-V specimens for the JMTR irradiation. Post irradiation tests for those specimens have been planned in the near future.

3. RESULTS

All results of fracture toughness tests performed in the ductile-to-brittle transition range are tabulated in Appendix.

3.1 JRQ unirradiated

Figure 1 shows K_{JC} values of test specimens fractured by cleavage mode in the transition range. At room temperature, cleavage fracture was not observed from any PCCv specimens, but from all 0.5TDCT and 1TCT specimens. There was also one PCCv specimen without cleavage fracture up to maximum load at -30 ℃. Specimen size and geometry of these specimens affected the upper limit of temperature indicating cleavage fracture by more than 50 ℃. When PCCv and 1T-CT data are compared at –80 ℃, it is seen that 1T-CT data are situated within the scatter range of PCCv data. J_{IC} value at 100 ℃ obtained from 1T-CT and 0.5T-DCT specimens by means of the JSME method is also indicated in the figure. Some data points of PCCv and compact specimens tested at upper transition temperature exceeded the J_{IC} value.

3.2 JRQ irradiated

Figure 2 shows all cleavage fracture toughness data of irradiated JRQ specimens. Test temperatures for five PCCv and six 0.5TDCT specimens, performed in the frame work of IAEA CRP-3, were sparse from 0 to 100 ℃. We tested additional irradiated PCCv specimens; twelve specimens around 17 ℃ and ten at 35 ℃ so that a statistical analysis could be done.

3.3 JSPS A533B-1

Figure 3 shows fracture toughness values from PCCv specimens of JSPS A533B-1 steel with a large number of database of compact specimens from 0.5T to 4T.[13] The database include –25, 0 and 25 ℃ data while PCCv were tested at 0 ℃. Obviously PCCv data show higher fracture toughness values than other compact specimen data. For this material, J_{IC} value at upper shelf temperature is not available.

3.4 Steel A

The cleavage fracture toughness data of Steel A are shown in Figure 4. The data includes some valid K_{IC} data from 4T-CT. The K_{IC} data locates nearly the lowest bound of the other data. The PCCv data show obviously higher K_{JC} values than K_{JC} of 1T-CT and K_{IC} of 4T-CT data. The upper shelf fracture toughness, J_{IC}, obtained by 1T-CT at 20 ℃ is indicated in the

specimens of the steels were encapsuled with ten Charpy-V specimens for the JMTR irradiation. Post irradiation tests for those specimens have been planned in the near future.

3. RESULTS

All results of fracture toughness tests performed in the ductile-to-brittle transition range are tabulated in Appendix.

3.1 JRQ unirradiated

Figure 1 shows K_{JC} values of test specimens fractured by cleavage mode in the transition range. At room temperature, cleavage fracture was not observed from any PCCv specimens, but from all 0.5TDCT and 1TCT specimens. There was also one PCCv specimen without cleavage fracture up to maximum load at -30 ℃. Specimen size and geometry of these specimens affected the upper limit of temperature indicating cleavage fracture by more than 50 ℃. When PCCv and 1T-CT data are compared at –80 ℃, it is seen that 1T-CT data are situated within the scatter range of PCCv data. J_{IC} value at 100 ℃ obtained from 1T-CT and 0.5T-DCT specimens by means of the JSME method is also indicated in the figure. Some data points of PCCv and compact specimens tested at upper transition temperature exceeded the J_{IC} value.

3.2 JRQ irradiated

Figure 2 shows all cleavage fracture toughness data of irradiated JRQ specimens. Test temperatures for five PCCv and six 0.5TDCT specimens, performed in the frame work of IAEA CRP-3, were sparse from 0 to 100 ℃. We tested additional irradiated PCCv specimens; twelve specimens around 17 ℃ and ten at 35 ℃ so that a statistical analysis could be done.

3.3 JSPS A533B-1

Figure 3 shows fracture toughness values from PCCv specimens of JSPS A533B-1 steel with a large number of database of compact specimens from 0.5T to 4T.[13] The database include –25, 0 and 25 ℃ data while PCCv were tested at 0 ℃. Obviously PCCv data show higher fracture toughness values than other compact specimen data. For this material, J_{IC} value at upper shelf temperature is not available.

3.4 Steel A

The cleavage fracture toughness data of Steel A are shown in Figure 4. The data includes some valid K_{IC} data from 4T-CT. The K_{IC} data locates nearly the lowest bound of the other data. The PCCv data show obviously higher K_{JC} values than K_{JC} of 1T-CT and K_{IC} of 4T-CT data. The upper shelf fracture toughness, J_{IC}, obtained by 1T-CT at 20 ℃ is indicated in the

figure. More than half of PCCv data at −50 ℃ exceeded the J_{IC} value.

3.5 Steel B

Figure 5 indicates the results of fracture toughness tests by specimens of Steel B. Some valid K_{IC} data from 4T-CT are also shown in this figure. The K_{IC} lies nearly lowest bound of the other data. Similarly to Steel A, PCCv data indicate higher toughness values than other CT data. The upper shelf fracture toughness, J_{IC}, obtained from 1T-CT at 20 ℃ is indicated in the figure. Several PCCv data at −80 ℃ exceeded the J_{IC} value.

4. DISCUSSION

4.1 Validity Limit for Cleavage Fracture Toughness Data

Cleavage fracture toughness values shown in Figures 1 to 5 were calculated by equations (1) and (2) without any limitation. However, due to relatively large yielding size compared to a specimen size, J-integral value at fracture can be invalid when it goes high. The limitation on J-integral value is described in some standards depending on the application and the related references. The major equations for the limitation of fracture toughness in some standards are described below.

(a) ASTM E1737[19] on standard test method for J-integral characterization of fracture toughness provides the following conditions to qualify J_{Qc} as J_c:

$$B, a_0, b_0 < \frac{J_{Qc}\sigma_Y}{200} \tag{4}$$

$$\Delta a < 0.2 + J_{Qc}/\alpha\,\sigma_Y, \quad \alpha \geqq 2 \tag{5}$$

where Δa is an amount of ductile crack growth.

This equation (4) is the same type as proposed by Anderson and Dodds[19] on specimen size requirements regarding a small scale yielding condition. When the specimen size satisfies the equation, a yielding condition in the specimen is considered as small scale yielding. Therefore J-integral value is valid for the fracture toughness of the material. For equation (5), the ductile crack extension before cleavage fracture is restricted to stretch zone width plus 0.2 mm. This limitation will be treated in section 4.5 with a fractographic study.

(b) Standard test method for fracture toughness within ductile brittle transition range by JSPS 129-committee;

$$b_0, B < \frac{J_C\sigma_Y}{25} \tag{6}$$

The equation (6) used in the JSPS method has the same coefficient as the validity

figure. More than half of PCCv data at −50 ℃ exceeded the J_{IC} value.

3.5 Steel B

Figure 5 indicates the results of fracture toughness tests by specimens of Steel B. Some valid K_{IC} data from 4T-CT are also shown in this figure. The K_{IC} lies nearly lowest bound of the other data. Similarly to Steel A, PCCv data indicate higher toughness values than other CT data. The upper shelf fracture toughness, J_{IC}, obtained from 1T-CT at 20 ℃ is indicated in the figure. Several PCCv data at −80 ℃ exceeded the J_{IC} value.

4. DISCUSSION

4.1 Validity Limit for Cleavage Fracture Toughness Data

Cleavage fracture toughness values shown in Figures 1 to 5 were calculated by equations (1) and (2) without any limitation. However, due to relatively large yielding size compared to a specimen size, J-integral value at fracture can be invalid when it goes high. The limitation on J-integral value is described in some standards depending on the application and the related references. The major equations for the limitation of fracture toughness in some standards are described below.

(a) ASTM E1737[19] on standard test method for J-integral characterization of fracture toughness provides the following conditions to qualify J_{Qc} as J_c:

$$B, a_0, b_0 < \frac{J_{Qc}\sigma_Y}{200} \tag{4}$$

$$\Delta a < 0.2 + J_{Qc}/\alpha\,\sigma_Y, \quad \alpha \geqq 2 \tag{5}$$

where Δa is an amount of ductile crack growth.

This equation (4) is the same type as proposed by Anderson and Dodds[19] on specimen size requirements regarding a small scale yielding condition. When the specimen size satisfies the equation, a yielding condition in the specimen is considered as small scale yielding. Therefore J-integral value is valid for the fracture toughness of the material. For equation (5), the ductile crack extension before cleavage fracture is restricted to stretch zone width plus 0.2 mm. This limitation will be treated in section 4.5 with a fractographic study.

(b) Standard test method for fracture toughness within ductile brittle transition range by JSPS 129-committee;

$$b_0, B < \frac{J_C\sigma_Y}{25} \tag{6}$$

The equation (6) used in the JSPS method has the same coefficient as the validity

criterion on the determination of a J_{IC} in the ASTM E813. The JSPS method also uses the equation (4) as a criterion of data correction in terms of specimen size requirements.

(c) ASTM draft test method for the determination of reference temperature for ferritic steels in the transition range;

$$K_{JC\_limit} = \sqrt{Eb_0\sigma_{ys}/30} \tag{7}$$

This equation can be expressed in a similar way to the previous equations (4) and (6).

$$b_0 < \frac{J_C\sigma_{ys}}{30} \tag{7'}$$

Referring equations (4) to (7'), the limitation on J-integral value at cleavage fracture can be expressed in the following form;

$$J_C < \frac{\{b_0 \text{ or } B\}\sigma_Y}{M} \tag{8}$$

M=25, 30, or 200.

For a PCCv specimen, the ligament size, b_0, is smaller than the specimen thickness, B. Therefore, b_0 is considered below as a key parameter for discussion of data validity.

Figures 1 to 5 include the J-integral limitation lines on the J-integral value of PCCv data for M=30 and 200. The J-limitation curves were calculated based upon the temperature dependence on yield strength of each material. As shown in the figures, many PCCv data are higher then the limitation. The latter case (M=200) is so much strict for the PCCv data that only one data of JRQ satisfied the limitation. On the other hand, no 1T-CT data exceeded the limitation. This means that PCCv specimens hardly satisfy the small scale yielding condition unless we perform fracture toughness tests at lower temperature.

For the case M=30 stipulated in the ASTM draft, more than half of PCCv data satisfied the J-limitation. The draft method requires at least six valid data on the J-limitation. In this study, we could take some valid data sets at the low test temperature regarding the number of data. However, when we need the temperature dependence of cleavage fracture toughness, the limitation on J-integral would be too strict for the use of PCCv specimens.

4.2 Specimen Size Effect on Cleavage Fracture Toughness

As is known well, a fracture toughness value from a small specimen can be higher than that from a large specimen. One of the reasons is that the small specimen has insufficient length in thickness to maintain a constraint of a crack tip by a certain level compared with a large size specimen or a real heavy-section structure. The ligament size of specimen is also an important factor to utilize a J-integral value as a valid parameter for describing the fracture. In addition to this, in the transition range, a statistical effect on cleavage fracture is apparent. This has been

explained by the weakest link theory that is based on the local inhomogeneity in the material. The theory treats the probability to find a particle that is located randomly in the material and that leads to the fracture of the specimen. This section of the paper describes the effect of specimen size and the effect of side-grooves (SG).

Figures 6 to 9 indicate cleavage fracture toughness values as a function of specimen net thickness. Figure 6 compares PCCv data tested with and without SG and 1T-CT data with SG of unirradiated JRQ tested at –80 ℃. The PCCv data without SG ranged most widely; the lowest point is even lower than the lowest point of 1T-CT data. The effect of specimen size is not so obvious in this case.

Figure 7 shows PCCv, 0.5T-CT and 1T-CT data with and without SG, and 2T-CT and 4T-CT data with SG of JSPS A533B-1 steel tested at 0 ℃. For this material, the effect of specimen size is apparent; PCCv data are higher than the other data from the other CT specimens. The 1T-CT and larger specimens tested with SG seem to provide approximately the same fracture toughness. This figure also shows the effect of SG. The highest data points of PCCv, 0.5T-CT and 1T-CT specimens without SG were higher than the highest of those specimens with SG. The data of PCCv without SG, however, provided lower data points in average than those with SG. Back to Figure 6, the average value of PCCv data without SG of JRQ was also slightly lower than those with SG. The reason is not clear, at this moment, why the effect of SG in PCCv specimen is different from larger CT specimens. A side-grooving is usually expected to make a crack front straight and avoid the loss of constraint near the crack front. Therefore, the fracture toughness value from a specimen with SG is expected to be lower than that of specimen without SG. The effect of SG in PCCv should be considered carefully when any specimen size correction is applied to the data.

Figures 8 and 9 indicate the specimen thickness dependence on cleavage fracture toughness of steels A and B tested at –80 ℃ and –110 ℃, respectively. Clearly PCCv data are higher than 1T-CT data for both steels. The lowest point of PCCv data of steel A is also higher than 1T-CT and 4T-CT data, while the lowest data of PCCv of steel B is almost coincident with that of 1T-CT and 4T-CT. In these cases, all PCCv specimens were machined to have SG. The effect of specimen size on the lowest toughness data is not clear. It may be necessary to obtain more PCCv data to compare the lowest data by means of the measured values.

4.3 Correction of Specimen Size Effect

To obtain a reliable fracture toughness value from a small size specimen, several correction schemes have been proposed. Wallin[9] has proposed the following equation for correcting specimen size applicable to pressure vessel steels;

$$K_{JC(y)} = K_{min} + (K_{JC(x)} - K_{min})(B_x/B_y)^{1/m} \quad (9)$$

where $K_{JC(x\ or\ y)}$: K_{JC} for specimens of another thickness, $B_{x\ or\ y}$

$K_{min} = 20\ MPa\sqrt{m}$

m = 4

Using this equation (9), K_{JC} values obtained from small specimens are usually adjusted to 1T-CT size using B_y=25 mm. This procedure has been discussed within the ASTM committee to make a standard for fracture toughness evaluation in the transition range. The adjusted value to 1T size is designated to K_{JC_1T}. This is because the 1T-CT specimens are usually used as a standard size specimen. Then the database is the largest one to describe the temperature dependence of cleavage fracture toughness that is mentioned afterwards. Figures 10 to 13 compare the raw data of PCCv, the size-adjusted data from PCCv to 1T size and the raw data of 1T-CT. The raw PCCv data were calculated according to the ASTM draft method. In addition, the raw PCCv data that exceed the limitation of equation (7) are excluded in this comparison.

The equation (9) is based on the weakest link theory. The theory assumes that the distribution of the fracture toughness values of a material can be described as a Weibull type statistics. Using three parameters, K_{min}(=20), m(=4) and K_0, the fracture probability based on Weibull statistics can be expressed by the following equation.

$$P_f = 1 - \exp\left(-\left(\frac{K_{JC\_1T} - K_{min}}{K_0 - K_{min}} \right)^m \right) = 1 - \exp\left(-\left(\frac{K_{JC\_1T} - 20}{K_0 - 20} \right)^m \right) \tag{10}$$

where P_f: Median ranking($= (i-0.3)/(N+0.4)$)

K_0: Fitting parameter

All data obtained by the same-type specimens at a certain temperature can be analyzed by these equations (9) and (10). This equation (10) has also been incorporated into the ASTM draft method to describe the statistics of cleavage fracture toughness. Taking natural logarithm of equation (10) twice, we obtain

$$\ln\left(\ln \frac{1}{1-P_f} \right) = m\left(\ln\left(K_{JC\_1T} - 20 \right) - \ln\left(K_0 - 20 \right) \right) \tag{11}$$

This means that the plot of data on Weibull-type graph is expressed by a linear line with a slope of m(=4). Figures 14 to 17 compare Weibull plots of PCCv data adjusted to 1T and 1T-CT data for all materials. PCCv adjusted data and 1T-CT data of unirradiated JRQ are in good agreement, as shown in Figure 14. However, the slopes of both linear-fit data, indicated by dotted lines, were 2.3 and 2.5 for PCCv adjusted data and 1T-CT data, respectively, which were much less than the theoretical value of four. Figure 15 shows the Weibull plots of PCCv data of irradiated JRQ. The slopes by linear fitting were 2.7 and 3.1 for the data tested at 17 ℃ and 35 ℃, respectively. The slopes were again smaller than the theoretical values. It is noted that the data scatter of JRQ remains very large after neutron irradiation.

On the other hand, the slope of 1TCT data of JSPS A533B-1 steel tested at 0 ℃, as shown in Figure 16, showed a large value, more than eight, which meant that the scatter of the

data was very small. PCCv and 2T-CT data were, however, agreed well although the slopes of linear fits were different; 3.6 for PCCv and 6.5 for 2T-CT.

Figures 17 and 18 show Weibull plots of steels A and B. In these cases, 1T-CT data were well fitted by means of a theoretical m value. PCCv adjusted data for both steels showed the same tendency as PCCv of JRQ, that is, the linear fit slopes were smaller than theoretical four. PCCv specimens of JRQ plotted in Figure 14 have no SG, while PCCv specimens of steels A and B in Figures 17 and 18 have 20 % of SG. The deviation of the slope from a theoretical value may not be the effect of SG for these materials. Material inhomogeneity itself may affect the scatter of the data. From this point of view, only PCCv data of JSPS A533B-1 steel was scattered theoretically because 1TCT data showed a surprising coherence. A fractographic study may be helpful to know what is actually happened at the crack tip. The results of fractographic observation will be mentioned later.

4.4 Temperature Dependence of Cleavage Fracture Toughness

The median value of the data can be obtained by K_0 from equation (10) and the following equation as a fracture probability P_f=0.5.

$$K_{JC\_1T(med)} = (K_0 - 20)[\ln(2)]^{1/4} + 20 \tag{12}$$

Using this median value, the temperature dependence of cleavage fracture toughness within the transition range is expressed by the following equation.

$$K_{JC\_1T(med)} = 30 + 70 \cdot \exp\{0.019 \cdot (T - T_0)\} \tag{13}$$

This equation has been established by statistical analyses using a huge database including unirradiated and irradiated RPV steels.[9] This equation, which is called a master curve, uniquely defines the cleavage fracture toughness transition curve. A reference temperature , T_0, can be calculated by

$$T_0 = T - \frac{1}{0.019} \cdot \ln\{(K_{JC\_1T(med)} - 30)/70\}. \tag{13'}$$

Table 4 lists the T_0 values obtained from materials used in this study. The censoring scheme described in the ASTM draft method was applied when the data set had any invalid data on equation (7). Figure 19 shows the values of T_0 based on the ASTM draft method as a function of specimen thickness. The values of T_0 from unirradiated JRQ and JSPS A533B-1 showed little effect on specimen thickness, while those of steels A and B gave some size effect. The T_0 values from PCCv data were 20 ℃ lower than those values from 1T-CT data for both steels A and B. The deviation of 20 ℃ is larger than the deviation of 5~10 ℃ reported for some RPV steels in reference (21). The reason of the deviation is not clear for the moment. Specimen sampled positions regarding the through-thickness inhomogeneity of the material were almost equal for PCCv and 1T-CT for these materials. Additional tests and the fractographic investigation might

help to understand the reason.

Based on Weibull statistics, tolerance bounds for the master curve can be drawn. Assuming the Weibull slope m=4, the third parameter K_{min}=20 and an infinite sampling size, a lower bound curve in the same form as equation (13) is defined. For example, 1% and 5% lower tolerance bounds are the following:

$$K_{JC\_1T(0.01)} = 23.5 + 24.5 \cdot \exp\{0.019 \cdot (T - T_0)\} \quad (14)$$

$$K_{JC\_1T(0.05)} = 25.4 + 37.8 \cdot \exp\{0.019 \cdot (T - T_0)\} \quad (15)$$

In addition, a standard deviation on a reference temperature T_0 can be calculated by the following:

$$\sigma = 18Z / \sqrt{N} \quad (16)$$

where N is the total number of specimen used to determine the value of T_0, Z a standard two-tail normal deviate. Figures 20 to 24 show master curves and 5% lower tolerance bound curves determined by equations (13) to (16) using valid PCCv data sets together with a margin adjusted lower bound curve. The master curve determined from PCCv data sets of unirradiated JRQ, which showed a large scatter in Figure 14, tends to overestimate the fracture toughness in the upper transition range as shown in Figure 20. Particularly 1T-CT and 0.5T-DCT data tested at RT are much lower than 5% tolerance bound. In this case, a 1% lower bound curve instead of 5% lower bound may be used to bound all data at the lowest points. The master curve shown in Figure 21 agrees well temperature dependence of 1T to 4T specimens of JSPS A533B-1 steel. Figure 21 indicates, however, that only a few data of 0.5T-CT lie under the 5% curve. Figures 22 and 23 for steels A and B also indicate that the master curves at higher temperature have a tendency to overestimate fracture toughness data. Although the lower bound curves again overvalue a few data points, the temperature dependence of the curves is in good agreement with the lowest points in the range tested.

Figure 24 shows the master curve and the lower tolerance bound for JRQ steel irradiated to 2×10^{19} n/cm^2 (E>1MeV). The T_0 value was determined by averaging values from two PCCv data sets tested at 17℃ and 35℃. The master curve again agrees well with the data. The lower bound also covers well up to the 0.5T-DCT data at 100℃. However, before irradiation, both PCCv and 1T-CT data of JRQ showed a large scatter and the lower bound curve could be expressed by the 1% tolerance bound. Therefore, the lower bound curve after irradiation should be the same tolerance bound curve of 1%. Figure 25 indicates the effect of irradiation on cleavage fracture toughness adjusted to 25 mm together with the master curves and 1% tolerance bounds. The shift of T_0 by irradiation to JRQ was 108 ℃. This shift is larger than the Charpy shift listed in Table 3 by about 20 ℃.

The equation (13) has a similar form to a K_{IC} curve in the ASME Sec. XI to describe the lower bound fracture toughness of RPV steels. The ASME K_{IC} lower bound curve is expressed by the following:

$$K_{IC} = 36.5 + 22.8 \cdot \exp\{0.036 \cdot (T - RT_{NDT})\} \quad (17)$$

In this case, we need an RT_{NDT} of the steel before and after irradiation to define the K_{IC} curve. The drop weight test can not be done after irradiation because the test requires relatively large size specimens. Therefore, Charpy impact results are used instead of the results of drop weight test to determine the irradiation effects. The adjusted RT_{NDT} value after neutron irradiation is then calculated with the Charpy shift added to the initial RT_{NDT}. The K_{IC} curve after irradiation is defined by an equation (17) using the adjusted value. This means that the irradiation effect on Charpy property and fracture toughness should be the same. The Charpy shift by irradiation for JRQ was less than the fracture toughness shift as mentioned above. The comparison of those shifts may not always be the same, because the strain rate is different from each other, and the specimen size effect and the scatter on fracture toughness can vary the shift of fracture toughness. To obtain more reliable fracture toughness data for the RPV integrity assessment, more detailed study using a larger database may be necessary.

The Japanese code on the method for the fracture toughness test and evaluation, JEAC 4206[22], also stipulates the lower bound toughness curve for the integrity assessment of RPV during a PTS transient. The curve can be defined as the lowest envelope of all the fracture toughness data points from the surveillance tests. The form of the curve is expressed by the following:

$$K_{JC} = 20.16 + 129.9 \cdot \exp\{0.0161 \cdot (T - T_{0J})\} \quad (18)$$

Applying equation (18) to the data of JRQ steel, we obtain the lower bound curves before and after irradiation, and hence the shift of the lower bound curves. Figure 26 indicates the JEAC curves before and after irradiation together with all test data. The lower bound curves agreed well with the data up to upper transition range, leading to a conservative evaluation. The shift of T_{0J} value by irradiation was calculated as 80 ℃. The shift according to the JEAC K_{IC} curve was less than the shift determined by the ASTM draft method. This may depend on the statistical treatment of the data. If we had more data from irradiated specimens or less data from unirradiated specimens, we might have got a larger shift by the JEAC method than Charpy shift. It is noted that the statistical analysis to evaluate the lowest fracture toughness is necessary when the number of data is insufficient regarding the data scatter.

4.5 Fractography for Measuring Stretch Zone Width and Ductile Crack Growth

The statistical analysis based on Weibull distribution showed that the data tends to be linear in the Weibull plots. However, at higher temperature, as ductile crack growth is expected, a fractographic study is necessary before Weibull analysis to account the crack growth. Then a stretch zone width (SZW) and the amount of ductile crack growth (Δa) were measured by means of a scanning electron microscope (SEM).

Figure 27 shows the relation between Jc and fractographic measures (SZW and Δa) for some selected specimens of steel A. All data except for one largest data point of Δa of

PCCv were satisfied with equation (5). From the measures by the fractography and a reference (23), it was assumed that a ductile crack initiated on a blunting line even if J-integral value had not reached the J_{IC} of the material yet. The blunting line used in this study was based on the recommendation in the JSME J_{IC} test method, as mentioned before. The ductile crack initiation point of a specimen was then defined as the point on the blunting line that corresponded to the SZW of the specimen. As shown in Figure 27, the Jc-R curve before cleavage fracture for each specimen was obtained by connecting the points of the initiation and the final fracture. The slope of the Jc-R curve have a similar trend to that of J-R curve determined at fully ductile regime (20°C). Figure 28 also shows the same type of results for the specimens of steel B. Therefore, the ductile crack initiation toughness J_{in} values can be defined as the initiation points on the blunting line. It is noted, however, that the J_{in} value should be less than J_{IC} value of the material because the J_{in} must saturate at the J_{IC}. The J_{in} values obtained can be converted to K_{Jin} values using equation (2). The K_{Jin} values may then be considered as the crack growth corrected fracture toughness. Since the K_{Jin} values are less than Jc values by the correction, the data scatter can also be less than that of Jc. Therefore, the statistical analysis of K_{Jin} values can be useful to determine the lower bound toughness. For the moment, the data from a fractographic study is insufficient to analyze the statistics.

The sites of cleavage fracture initiation were also observed by SEM. Cleavage initiation sites in fracture surface tested at the lowest temperatures were not clear but tended to be small in size and large numbers. On the other hand, at higher temperature, the sites were clearly observed at some distance from the ductile crack front. These observations seem to be similar to a two criteria model described by Landes et al.[24], i.e., at relatively low temperature region a fracture initiation is based on the critical damage accumulation, and at higher temperature a fracture occurs according to the weakest link theory. Figure 29 shows relations of Jc values and the distances, X, from ductile crack front to cleavage fracture initiation site. Figure 29 also indicates an estimated maximum stress region in front of a crack.[25] From the results shown in the figure, it is seen that the initiation site in a PCCv specimen after a large deformation tends to saturate at ~200 micron. This may be explained the loss of constraint at the crack front of the PCCv specimen. The stress distribution at the crack front of a PCCv specimen starts to go away from a theory such as the field of HRR singularity[26, 27] at a certain deformation level. The use of J-integral is normally limited up to the deformation level. However, a fractographic study can be useful for the understanding of a cleavage fracture, such as the determination of a microscopic critical fracture stress at a cleavage initiation site. Further study on this matter is necessary.

5. SUMMARY AND CONCLUSIONS

To establish the method to evaluate fracture toughness values in the transition region, fracture toughness tests using PCCv to 4T-CT specimens were performed. Although post

PCCv were satisfied with equation (5). From the measures by the fractography and a reference (23), it was assumed that a ductile crack initiated on a blunting line even if J-integral value had not reached the J_{IC} of the material yet. The blunting line used in this study was based on the recommendation in the JSME J_{IC} test method, as mentioned before. The ductile crack initiation point of a specimen was then defined as the point on the blunting line that corresponded to the SZW of the specimen. As shown in Figure 27, the Jc-R curve before cleavage fracture for each specimen was obtained by connecting the points of the initiation and the final fracture. The slope of the Jc-R curve have a similar trend to that of J-R curve determined at fully ductile regime (20°C). Figure 28 also shows the same type of results for the specimens of steel B. Therefore, the ductile crack initiation toughness J_{in} values can be defined as the initiation points on the blunting line. It is noted, however, that the J_{in} value should be less than J_{IC} value of the material because the J_{in} must saturate at the J_{IC}. The J_{in} values obtained can be converted to K_{Jin} values using equation (2). The K_{Jin} values may then be considered as the crack growth corrected fracture toughness. Since the K_{Jin} values are less than Jc values by the correction, the data scatter can also be less than that of Jc. Therefore, the statistical analysis of K_{Jin} values can be useful to determine the lower bound toughness. For the moment, the data from a fractographic study is insufficient to analyze the statistics.

The sites of cleavage fracture initiation were also observed by SEM. Cleavage initiation sites in fracture surface tested at the lowest temperatures were not clear but tended to be small in size and large numbers. On the other hand, at higher temperature, the sites were clearly observed at some distance from the ductile crack front. These observations seem to be similar to a two criteria model described by Landes et al.[24], i.e., at relatively low temperature region a fracture initiation is based on the critical damage accumulation, and at higher temperature a fracture occurs according to the weakest link theory. Figure 29 shows relations of Jc values and the distances, X, from ductile crack front to cleavage fracture initiation site. Figure 29 also indicates an estimated maximum stress region in front of a crack.[25] From the results shown in the figure, it is seen that the initiation site in a PCCv specimen after a large deformation tends to saturate at ~200 micron. This may be explained the loss of constraint at the crack front of the PCCv specimen. The stress distribution at the crack front of a PCCv specimen starts to go away from a theory such as the field of HRR singularity[26, 27] at a certain deformation level. The use of J-integral is normally limited up to the deformation level. However, a fractographic study can be useful for the understanding of a cleavage fracture, such as the determination of a microscopic critical fracture stress at a cleavage initiation site. Further study on this matter is necessary.

5. SUMMARY AND CONCLUSIONS

To establish the method to evaluate fracture toughness values in the transition region, fracture toughness tests using PCCv to 4T-CT specimens were performed. Although post

irradiation tests have finished only for JRQ, the following conclusion were drawn from the tests of four types of Japanese RPV steels and their analysis;

(1) The specimen size effect was seen between PCCv and 1T-CT data, particularly from steel A.
(2) The size effect adjustment for the median value based on the weakest link theory was not enough to obtain an equivalent value from a PCCv specimen to a large specimen.
(3) The data scatters of some data sets for all materials were analyzed by a Weibull type statistics. Experimantal values for the Weibull slope tend to be slightly less than the theoretical value of four, in particular, for JRQ.
(4) The fracture toughness transition curve was evaluated by means of the master curve approach. The master curve determined by PCCv data tends to go higher at the upper transition range than 1T-CT data.
(5) According to the master curve, the shift of the curve by irradiation was evaluated to be somewhat greater than the Charpy 41J shift.
(6) JEAC type lower bound toughness curves were also evaluated for JRQ data before and after irradiation. The shift obtained by the JEAC curve method was less than the shift of the master curve and even the Charpy shift.
(7) It was found through a fractographic study that a ductile crack growth preceding a cleavage fracture was the same tendency as the upper shelf J-R curve, and could be corrected to evaluate a conservative fracture toughness. The fractographic study also revealed that there might be the difference in the stress distribution in front of a crack between PCCv and 1T-CT specimens.

ACKNOWLEDGMENTS

The part of this work has been supported by the Science and Technology Agency of Japan. The authors would like to thank Dr. K. Shibata and Mr. Y. Nishiyama, Japan Atomic Energy Research Institute for their encouragement and helpful discussion, and many staffs at Hot Laboratory of JAERI for their careful testing of irradiated specimens. They are also grateful to Dr. T. Iwadate and Dr. Y. Tanaka of the Japan Steel Works, Ltd. for providing the JSPS A533B-1 material. The tests of PCCv specimens of JSPS A533B-1 were done at SCK/CEN during the period that one of the authors had stayed there.

irradiation tests have finished only for JRQ, the following conclusion were drawn from the tests of four types of Japanese RPV steels and their analysis;

(1) The specimen size effect was seen between PCCv and 1T-CT data, particularly from steel A.
(2) The size effect adjustment for the median value based on the weakest link theory was not enough to obtain an equivalent value from a PCCv specimen to a large specimen.
(3) The data scatters of some data sets for all materials were analyzed by a Weibull type statistics. Experimantal values for the Weibull slope tend to be slightly less than the theoretical value of four, in particular, for JRQ.
(4) The fracture toughness transition curve was evaluated by means of the master curve approach. The master curve determined by PCCv data tends to go higher at the upper transition range than 1T-CT data.
(5) According to the master curve, the shift of the curve by irradiation was evaluated to be somewhat greater than the Charpy 41J shift.
(6) JEAC type lower bound toughness curves were also evaluated for JRQ data before and after irradiation. The shift obtained by the JEAC curve method was less than the shift of the master curve and even the Charpy shift.
(7) It was found through a fractographic study that a ductile crack growth preceding a cleavage fracture was the same tendency as the upper shelf J-R curve, and could be corrected to evaluate a conservative fracture toughness. The fractographic study also revealed that there might be the difference in the stress distribution in front of a crack between PCCv and 1T-CT specimens.

ACKNOWLEDGMENTS

The part of this work has been supported by the Science and Technology Agency of Japan. The authors would like to thank Dr. K. Shibata and Mr. Y. Nishiyama, Japan Atomic Energy Research Institute for their encouragement and helpful discussion, and many staffs at Hot Laboratory of JAERI for their careful testing of irradiated specimens. They are also grateful to Dr. T. Iwadate and Dr. Y. Tanaka of the Japan Steel Works, Ltd. for providing the JSPS A533B-1 material. The tests of PCCv specimens of JSPS A533B-1 were done at SCK/CEN during the period that one of the authors had stayed there.

REFERENCES

(1) ASME Boiler and Pressure Vessel Code, Section XI, "Inservice Inspection of Nuclear Power Plant," American Society for Mechanical Engineers, 1995.

(2) Japanese Electric Association, "Methods of surveillance tests for structural materials of nuclear reactors," JEAC 4201-1991. (in Japanese)

(3) R. Nanstad et al., "Irradiation Effects on Fracture Toughness of Two High-Copper Submerged-arc Welds, HSSI Series 5," NUREG/CR-5913 Vol.1, October 1992, U.S.NRC.

(4) K. Wallin et al., "Beyond the Charpy - Improved toughness predictions and advanced surveillance," presented at Radiation Damage and Embrittlement in Pressure Vessel Steels - IGRDM Open Workshop, Santa Barbara, May 6, 1994.

(5) M.T. Miglin, et al., "Analysis of Results from the MPC/JSPS Round Robin Testing Program in the Ductile-to-Brittle Transition Region," Fracture Mechanics: Twenty-fourth Volume, ASTM STP 1207, J.D. Landes, D. E. McCabe and J. A. M. Boulet, Eds., Americal Society for Testing and Materials, Philadelphia, 1995, pp. 342-354.

(6) T. Iwadate et al., "An Analysis of Elastic-Plastic Fracture Toughness Behavior for JIC Measurement in the Transition Region," Elastic-Plastic Fracture: Second Symposium, Volume II-Fracture Resistance Curves and Engineering Applications, ASTM STP 803, American Society for Testing and Materials, 1983, pp. II-531-II-561.

(7) K. Wallin, "The Scatter in K_{IC}-Results," Engineering Fracture Mechanics, Vol. 19, No.6, pp.1085-1093, 1984.

(8) J.D. Landes and D.H. Shaffer, "Statistical Characterization of Fracture in the Transition region," Fracture Mechanics: Twelfth Conference, ASTM STP 700, American Society for Testing and Materials, 1980, pp. 368-382.

(9) K. Wallin, "Irradiation Damage Effects on the Fracture Toughness Transition Curve Shape for Reactor Pressure Vessel Steels," International Journal of Pressure Vessel and Piping, 55(1993) pp.61-79.

(10) ASTM Draft 13, "Test Method for The Determination of Reference Temperature, T0, for Ferritic Steels in the Transition Range," Rev. 7-1-96, ASTM.

(11) K. Onizawa et al., "JAERI contribution for the IAEA coordinated research program phase III on optimizing of reactor pressure vessel surveillance programmes and their analysis," JAERI-M 93-201, Japan Atomic Energy Research Institute (October 1993).

(12) CRP Sub-Committee, "Manufacturing History and Mechanical Properties of Japanese Materials Provided for The International Atomic Energy Agency," Japan Welding Engineering Society, Oct. 1986.

(13) JSPS 129 Committee, "Standard Test Method for Fracture Toughness within Ductile-Brittle Transition Range," Japan Society for Promoting Science, 1995.

(14) R. Chaouadi, "Fracture Toughness Measurements in the Transition Regime Using Small Size Samples," Small Specimen Test Techniques, ASTM STP 1329, W. R. Corwin, S. T.

Rosinski, and E. van Walle, Eds., American Society for Testing and Materials, Philadelphia, 1997, to be published.

(15) ASTM E399-83, "Standard Test Method for Plane-Strain Fracture Toughness of Metallic Materials," Annual Book of ASTM Standards, Vol.03.01, American Standard for Testing and Materials, 1983.

(16) ASTM E813-89, "Standard Test Method for J_{IC}, A Measure of Fracture Toughness," Annual Book of ASTM Standards, Vol.03.01, American Standard for Testing and Materials, 1989.

(17) JSME S001-1992, "Standard Method of Test for Elastic-Plastic Fracture Toughness J_{IC} (Supplement, 1st Edition)," The Japan Society of Mechanical Engineers, Feb., 1992.

(18) M. Nevalainen and R. Dodds, "Numerical Investigation of 3-D Constraint Effects on Brittle Fracture in SE(B) and C(T) Specimens," NUREG/CR-6317, UILU-ENG-95-2001, July 1996.

(19) ASTM E1737-96, "Standard Test Method for J-Integral Characterization of Fracture Toughneass," Annual Book of ASTM Standards, Vol.03.01, American Standard for Testing and Materials, 1996.

(20) T. Anderson and R. Dodds, "Specimen Size requirements for Fracture Toughness Testing in the Ductile-Brittle Transition Region," Journal of Testing and Evaluation, Vol. 19, 1991, pp. 123-134.

(21) K. Wallin, "Validity of Small Specimen Fracture Toughness Estimates Neglecting Constraint Corrections," Constraint Effects in Fracture Theory and Applications: Second Volume, ASTM STP 1244, M. Kirk and Ad Bakker, Eds. American Society for Testing and Materials, Philadelphia, 1995.

(22) Japanese Electric Association, "Fracture Toughness Test Methods for Nuclear Power Plant Components," JEAC 4206-1991. (in Japanese)

(23) H. Kobayashi, et al., "Evaluation of Brittle Fracture Toughness and Ductile Crack Growth in the Transition Region," Trans. JSME, Vol. 52, No. 473, 1986 (in Japanese).

(24) J. D. Landes, "A Two Criteria Statistical Model for Transition fracture toughness," Fatigue Fract. Engng. Mater. Struct. vol. 16, No. 11, pp. 1161-1174, 1993.

(25) K. Onizawa, unpublished work.

(26) J. W. Hutchinson, "Singular Behavior at the End of a Tensile Crack in a Hardening Material," Journal of the Mechanics and Physics of Solids, 16, pp. 13-31, 1968.

(27) J. R. Rice and G. F. Rosengren, "Plane Strain Deformation Near a Crack Tip in a Power Low Hardening Material," Journal of the Mechanics and Physics of Solids, 16, pp. 1-12, 1968.

Table 1 Chemical compositions of materials used in this study.

(wt.%)

Material	C	Si	Mn	P	S	Ni	Cr	Cu	Mo
JRQ	0.18	0.24	1.42	0.017	0.004	0.84	0.12	0.14	0.51
JSPS A533B-1	0.24	0.41	1.52	0.028	0.023	0.43	0.08	-	0.49
Steel A	0.19	0.30	1.30	0.015	0.010	0.68	0.17	0.16	0.53
Steel B	0.19	0.19	1.43	0.004	0.001	0.65	0.13	0.04	0.50

Table 2 Material properties at room temperature of materials used in this study.

Material	σ_{ys} (MPa)	σ_{uts} (MPa)	Elongation (%)	Note
JRQ	477	615	22.2	
JSPS A533B-1	504	692	20.2	Ref. (13)
Steel A	469	612	26.4	
Steel B	462	597	24.9	

Table 3 Neutron irradiation effect on material properties of JRQ.

Item	Fast Neutron Fluence	Irradiation Temperature	Index	Shift / Increase
Charpy shift	~2.3x10^{19} n/cm^2	~291 ℃	ΔT_{41J}	85 ℃
			ΔT_{68J}	89 ℃
			$\Delta T_{50\%}$	86 ℃
Hardening	~1.6x10^{19} n/cm^2	~288 ℃	$\Delta \sigma_{ys}$	117 MPa
			$\Delta \sigma_{uts}$	107 MPa
			Δ Elong.	-2.7 %
	~2.2x10^{19} n/cm^2	~286 ℃	Δ Hv(98N)	41 VHN

Table 4 Comparison of the values of T_0 determined according to the ASTM draft method.

Material	JRQ unirradiated					
Specimen	B(mm)	T_0(℃)	N	r	Temp. (℃)	SG(%)
PCCv	10.0	−73.8	16	14	−80	0
PCCv	10.0	−66.0	8	8	−80	20
PCCv	10.0	−63.3	16	9	−50	0
1TCT	25.0	−66.4	6	6	−80	20

Material	JRQ irradiated					
Specimen	B(mm)	T_0(℃)	N	r	Temp. (℃)	SG(%)
PCCv	10.0	31.9	12	11	17	0
PCCv	10.0	47.8	10	10	35	0

Material	JSPS A533B-1					
Specimen	B(mm)	T_0(℃)	N	r	Temp. (℃)	SG(%)
PCCv	10.0	−1.1	10	7	0	0
PCCv	10.0	−	10	4	0	20
0.5TCT	12.7	7.8	16	16	−25	20
0.5TCT	12.7	19.1	17	17	0	20
0.5TCT	12.7	6.8	6	6	0	0
0.5TCT	12.7	7.1	12	11	25	20
1TCT	25.4	9.7	18	18	−25	20
1TCT	25.4	20.4	18	18	0	20
1TCT	25.4	7.7	6	6	0	0
1TCT	25.4	18.6	12	12	25	20
2TCT	50.8	5.4	6	6	0	20

Material	Steel A					
Specimen	B(mm)	T_0(℃)	N	r	Temp. (℃)	SG(%)
PCCv	10.0	−86.6	10	7	−80	20
1TCT	25.0	−66.9	12	12	−80	20
1TCT	25.0	−66.9	12	12	−50	20

Material	Steel B					
Specimen	B(mm)	T_0(℃)	N	r	Temp. (℃)	SG(%)
PCCv	10.0	−113.0	10	8	−110	20
1TCT	25.0	−102.4	12	12	−110	20
1TCT	25.0	−92.4	12	12	−80	20

B: Specimen thickness
N: Total number of data used
r: Number of valid data
SG: Side grooving

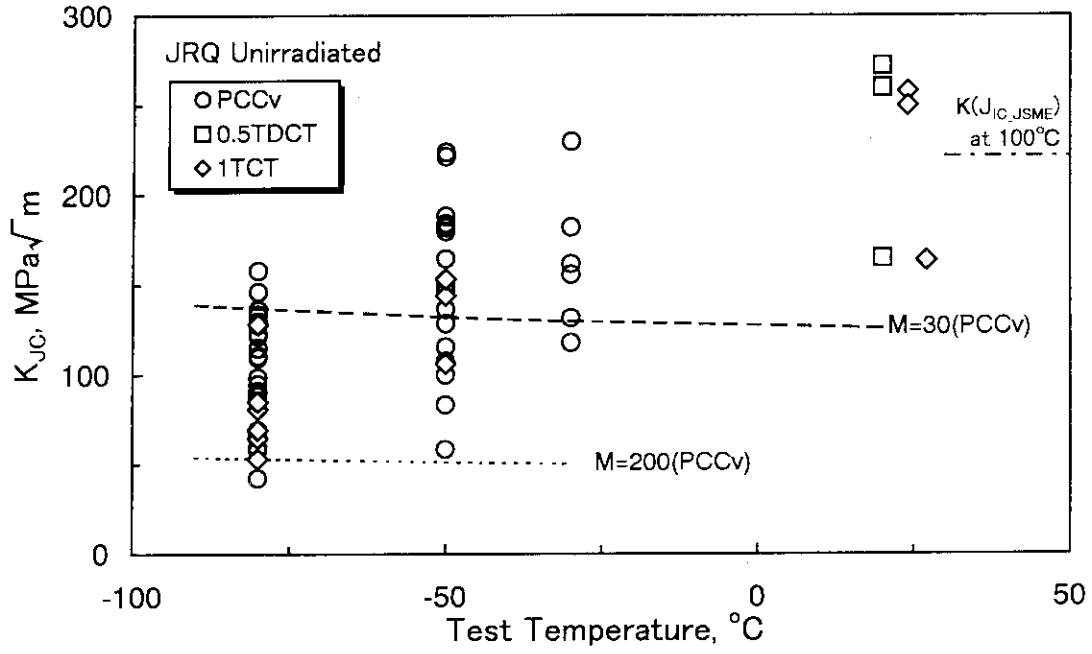

Figure 1--Fracture toughness test results of unirradiated JRQ steel.

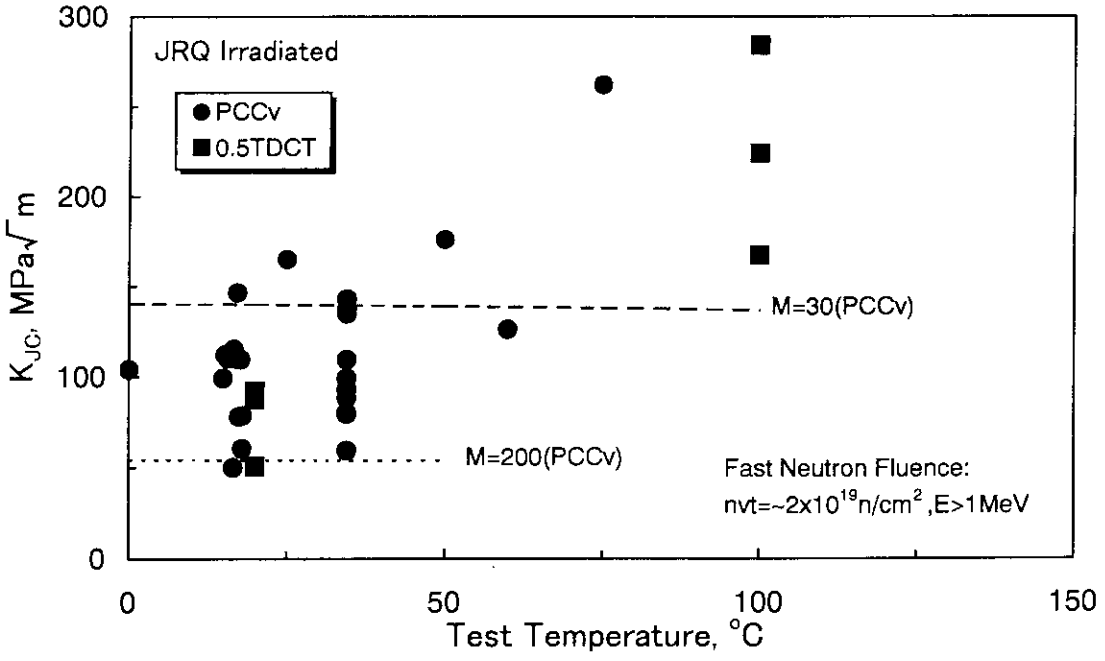

Figure 2--Fracture toughness test results of irradiated JRQ steel.

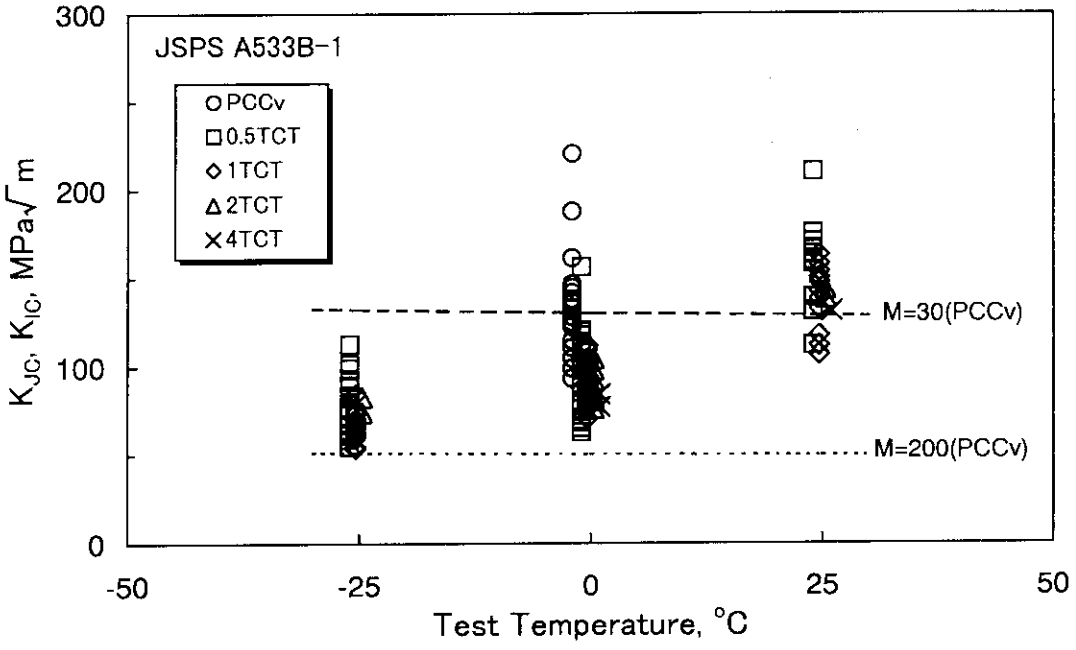

Figure 3--Fracture toughness test results of JSPS A533B-1 steel.

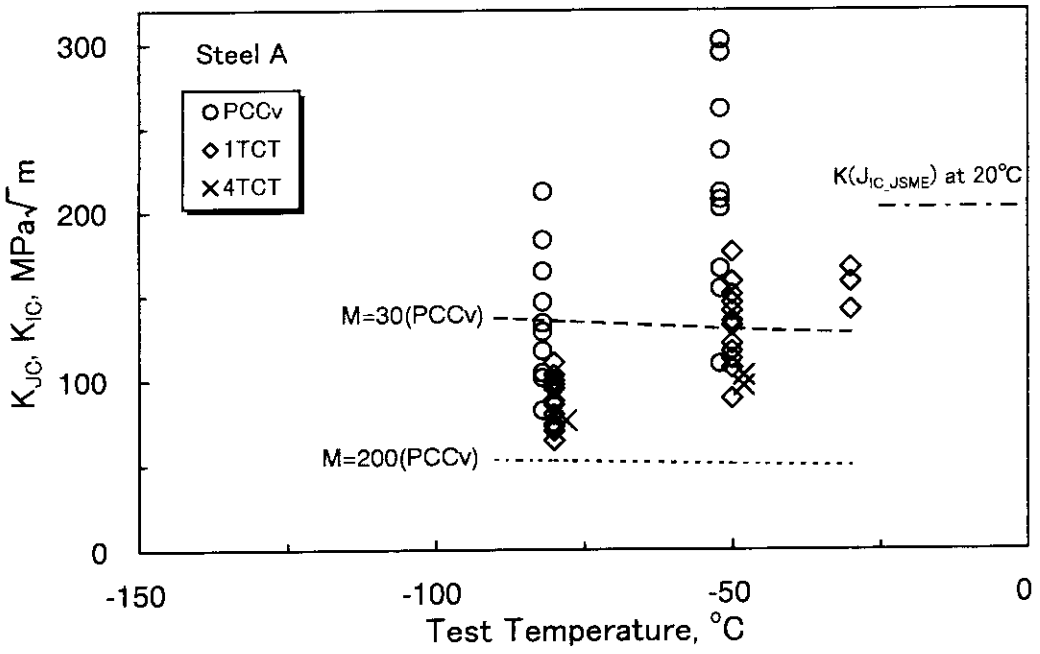

Figure 4--Fracture toughness test results of Steel A.

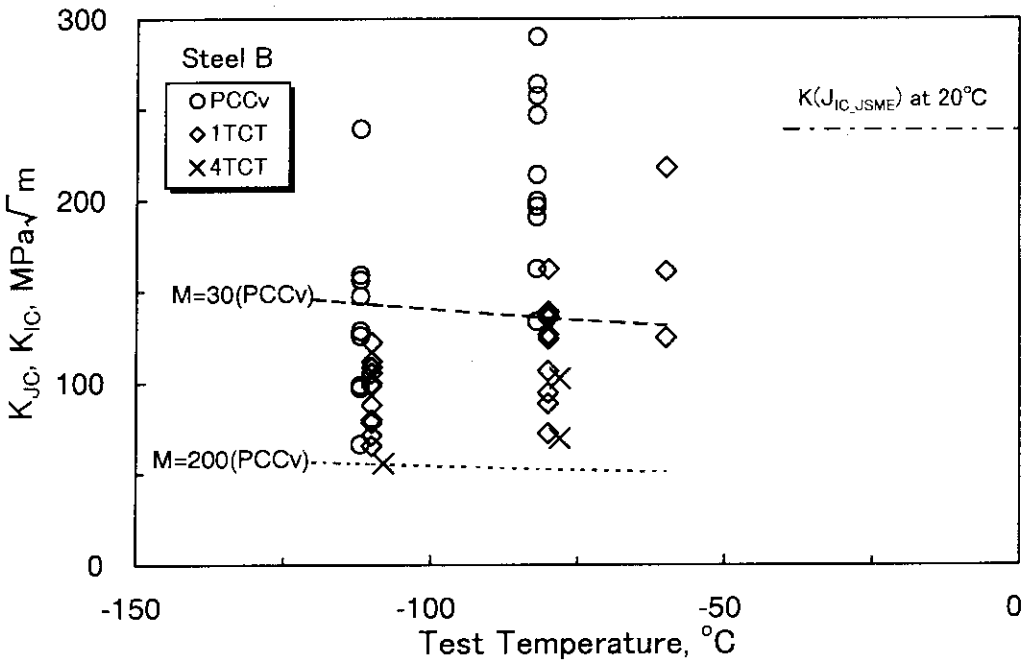

Figure 5--Fracture toughness test results of Steel B.

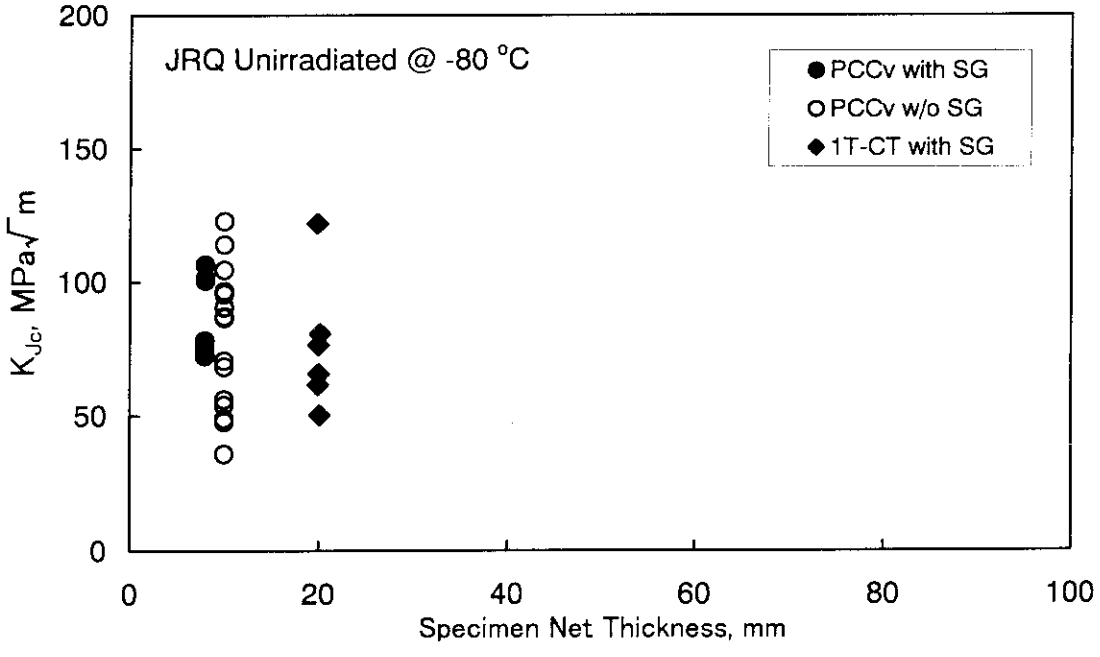

Figure 6--Fracture toughness values of unirradiated JRQ tested at –80 ℃ as a function of specimen net thickness.

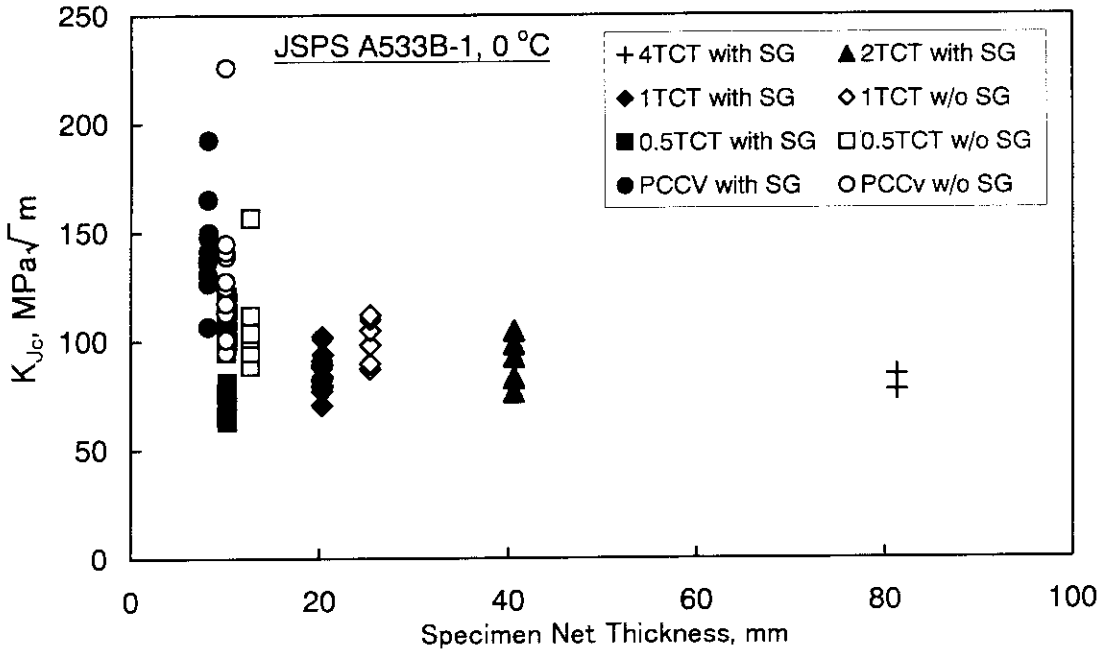

Figure 7--Fracture toughness values of JSPS A533B-1 tested at 0 ℃ as a function of specimen net thickness.

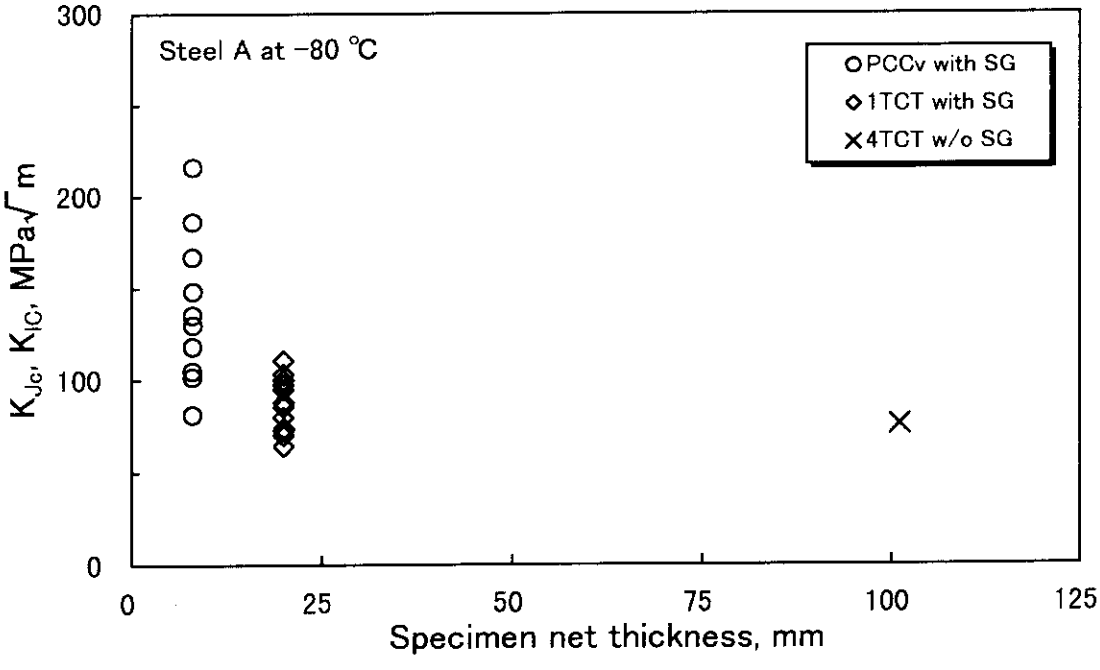

Figure 8--Fracture toughness values of Steel A tested at −80 ℃ as a function of specimen net thickness.

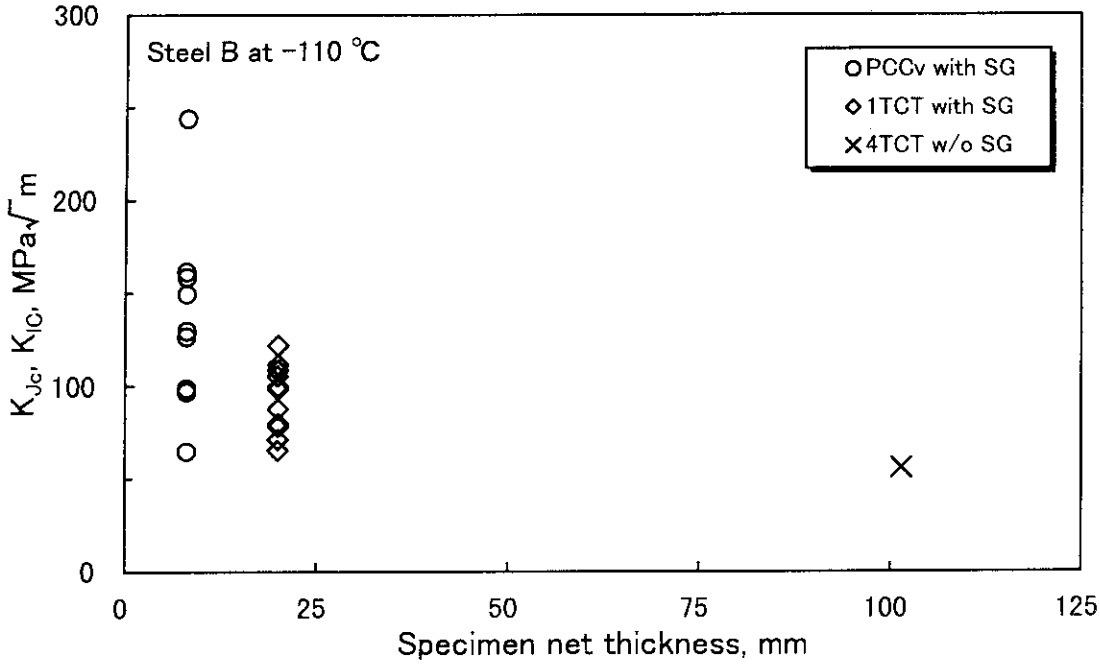

Figure 9--Fracture toughness values of Steel B tested at –110 ℃ as a function of specimen net thickness.

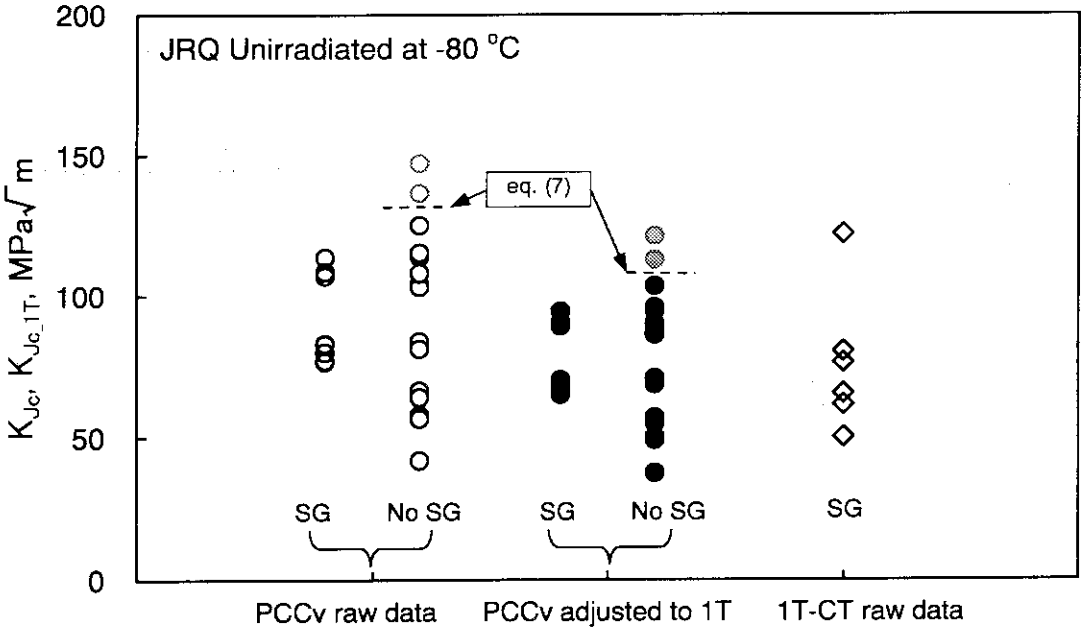

Figure 10--Comparison of PCCv data with and without the adjustment to 1T size and 1T-CT data of unirradiated JRQ at –80 ℃.

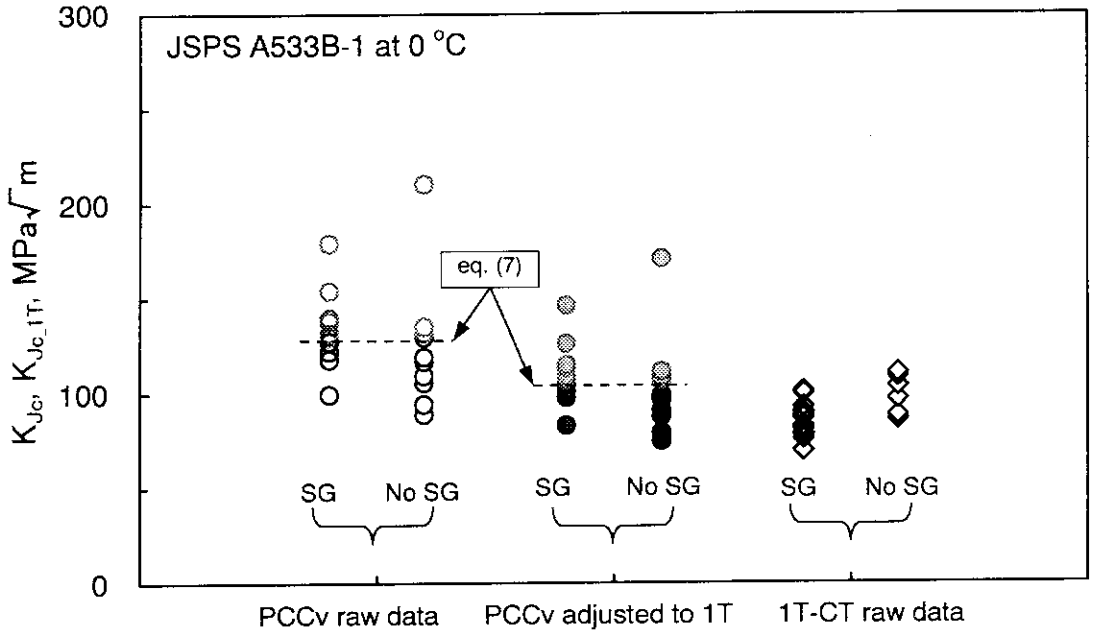

Figure 11--Comparison of PCCv data with and without the adjustment to 1T size and 1T-CT data of JSPS A533B-1 at 0 ℃.

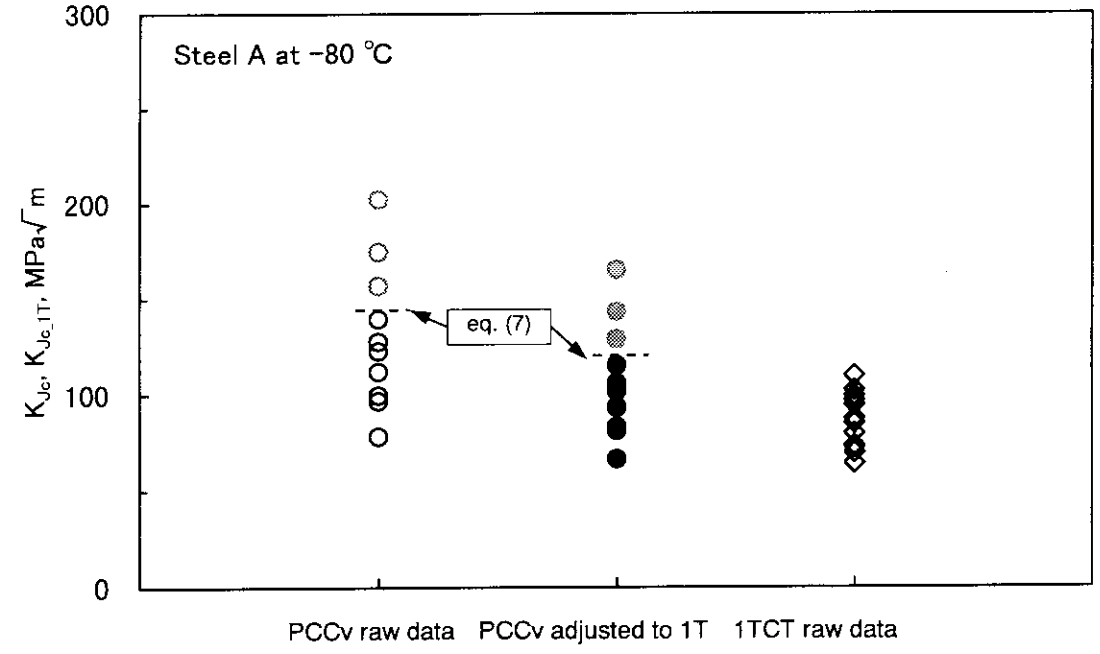

Figure 12--Comparison of PCCv data with and without the adjustment to 1T size and 1T-CT data of Steel A at –80 ℃.

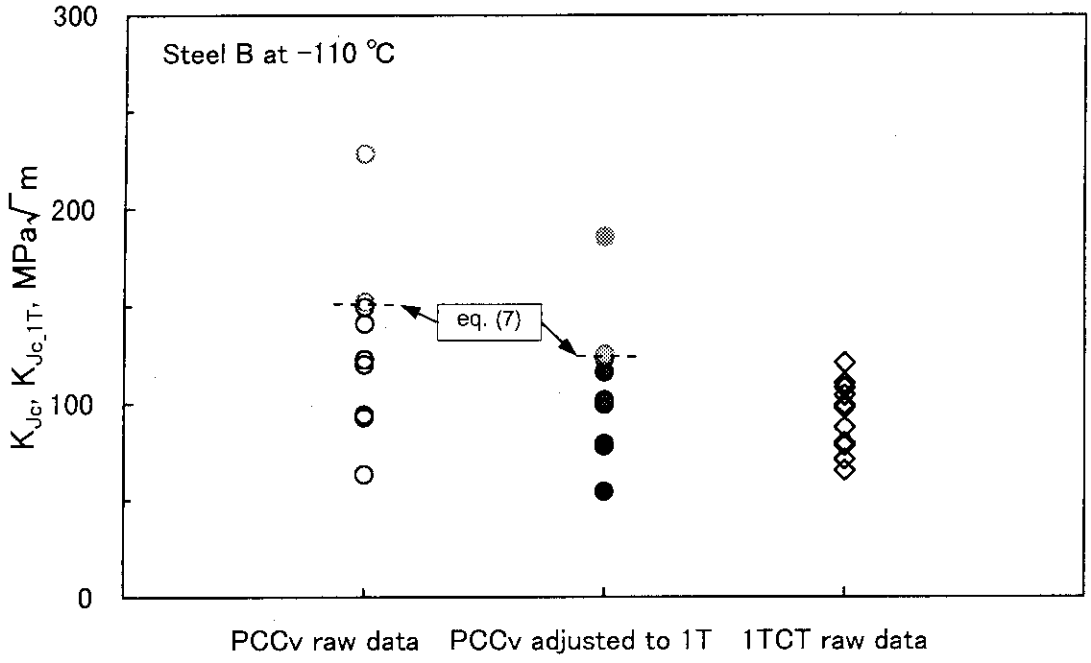

Figure 13--Comparison of PCCv data with and without the adjustment to 1T size and 1T-CT data of Steel B at –110 ℃.

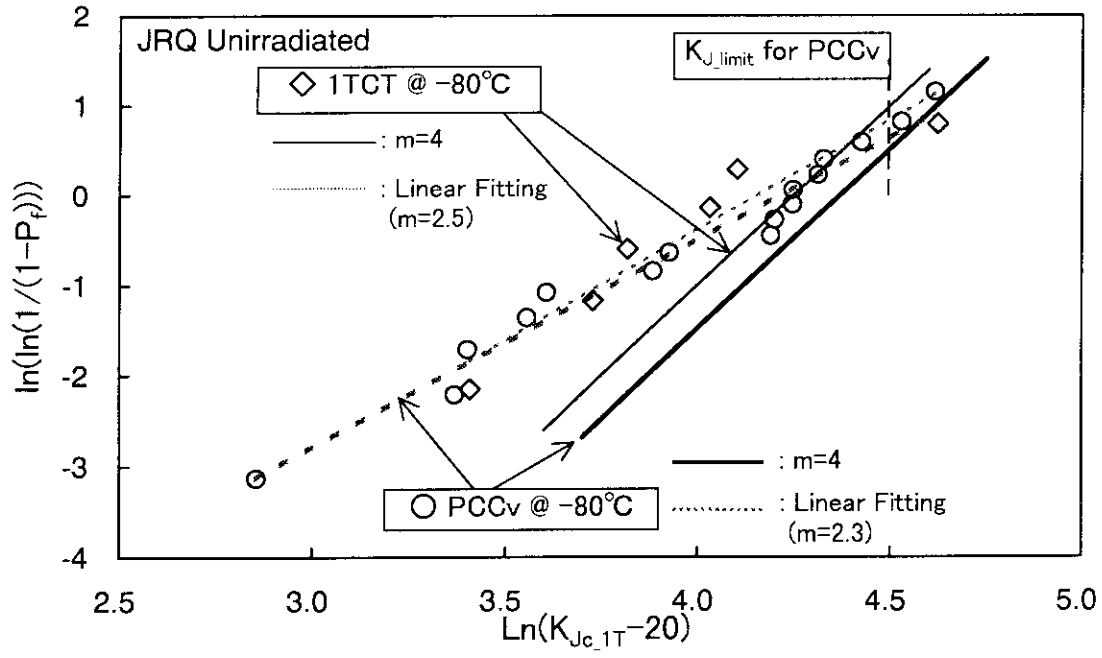

Figure 14--Weibull plots of unirradiated JRQ data at –80 ℃.

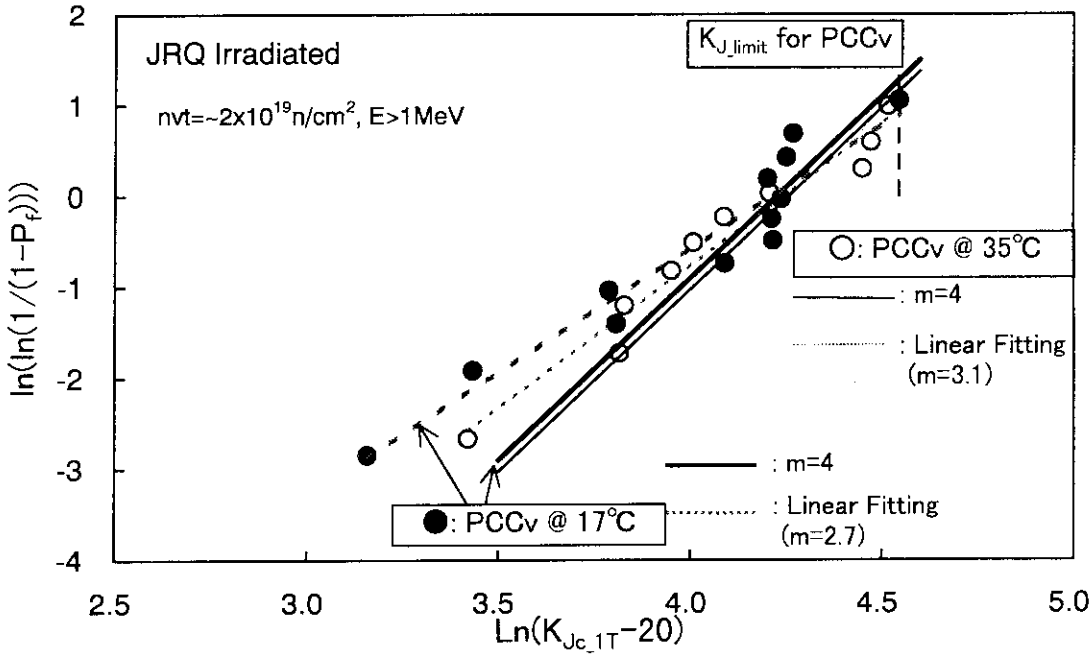

Figure 15--Weibull plots of irradiated JRQ data at 17 and 35 ℃.

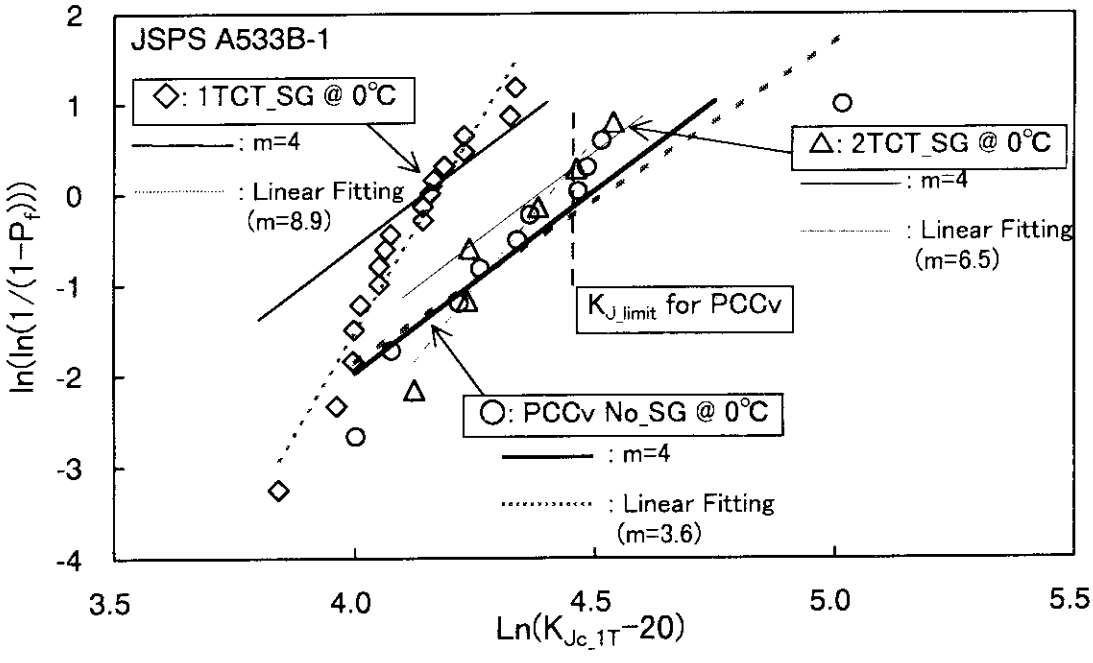

Figure 16--Weibull plots of JSPS A533B-1 data at 0 ℃.

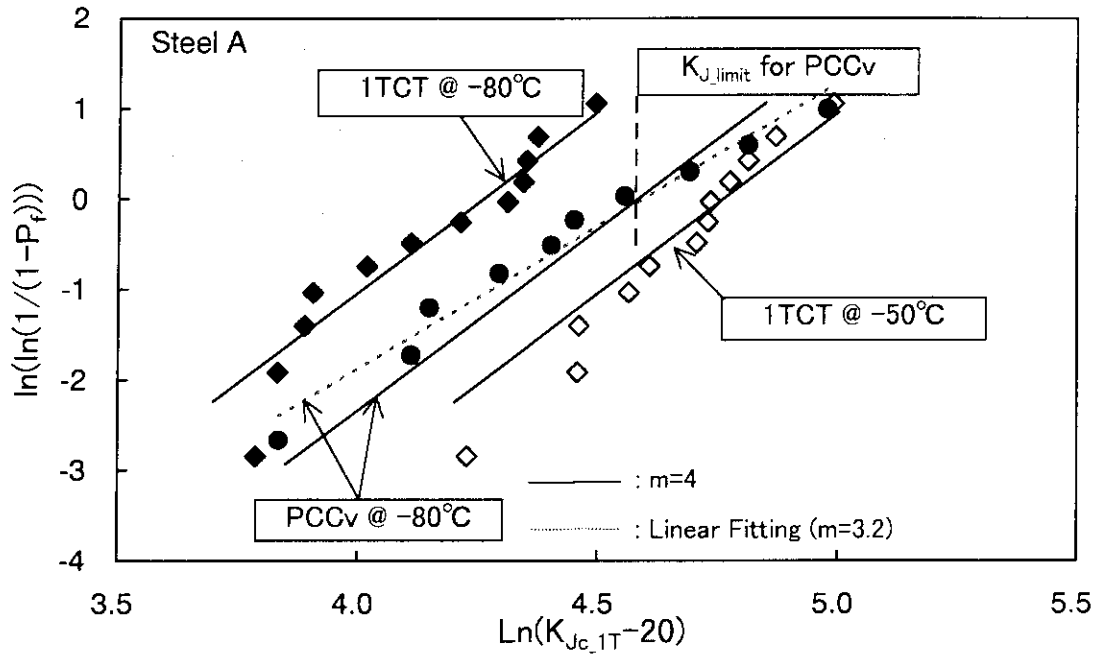

Figure 17--Weibull plots of Steel A data at –80 ℃ and –50 ℃.

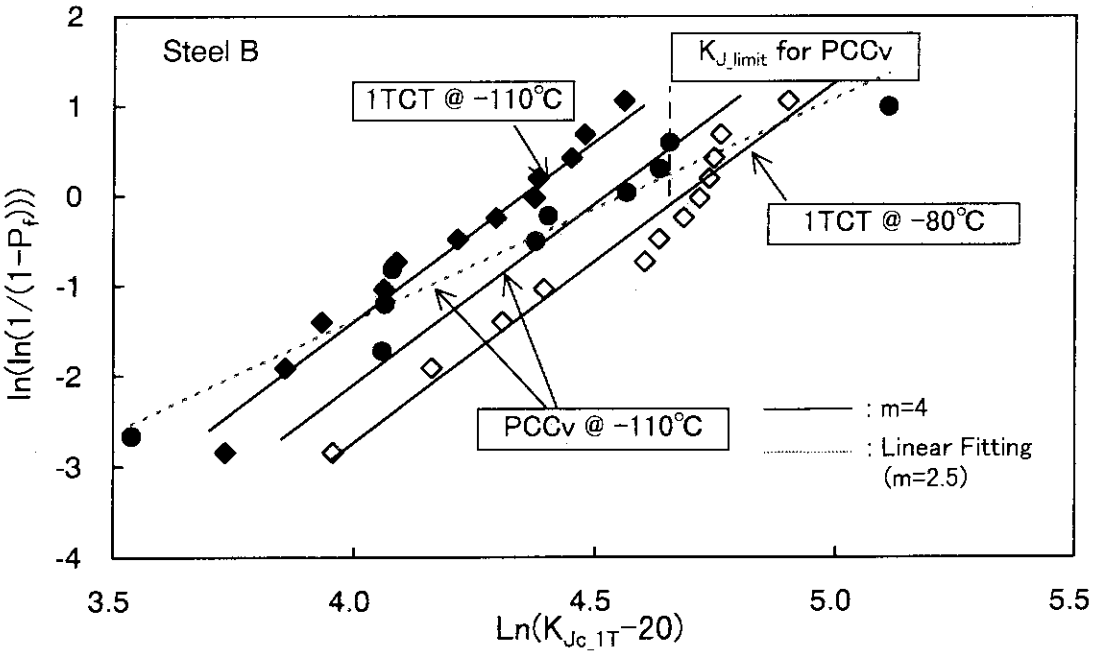

Figure 18--Weibull plots of Steel B data at –110 and –80 ℃.

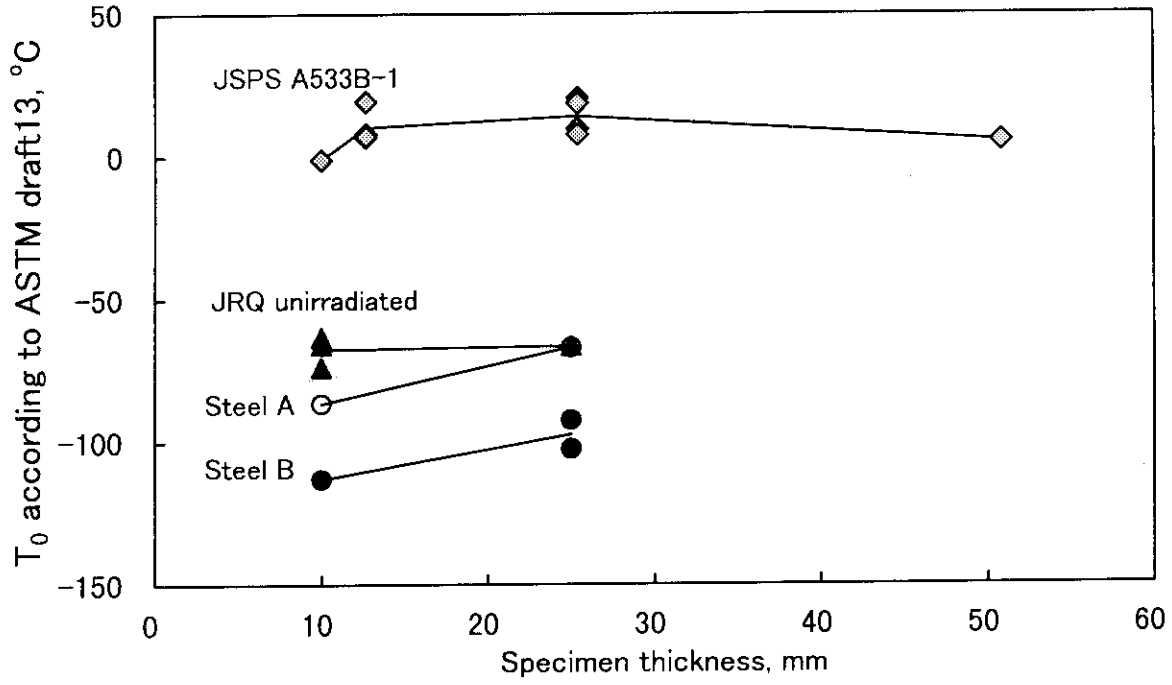

Figure 19 -- Comparison of reference temperature, T_0, according to the ASTM draft method as a function of specimen gross thickness.

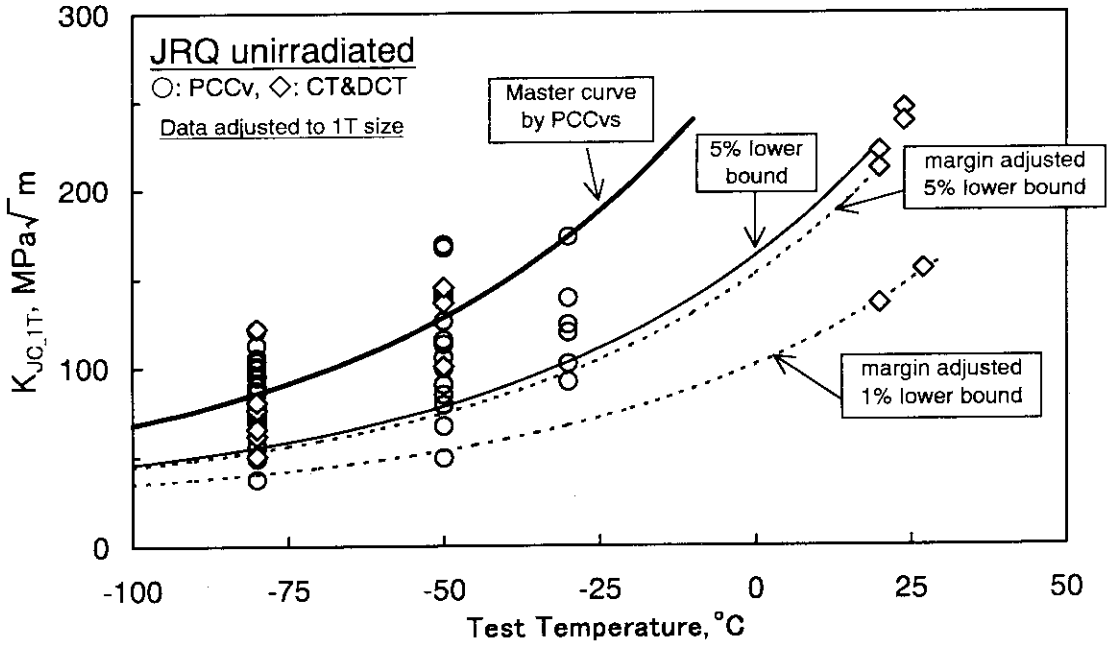

Figure 20--Size adjusted data to 1T, the master curve and lower bound curves determined by PCCv data of unirradiated JRQ steel.

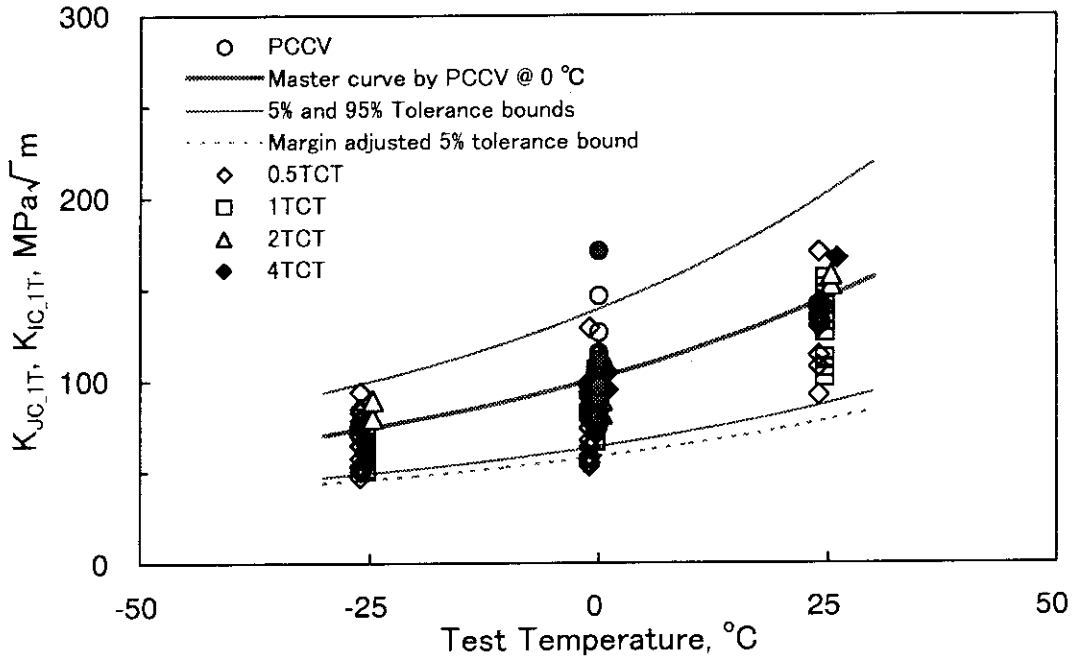

Figure 21--Size adjusted data to 1T, the master curve and tolerance bound curves determined by PCCv data of JSPS A533B-1 steel.

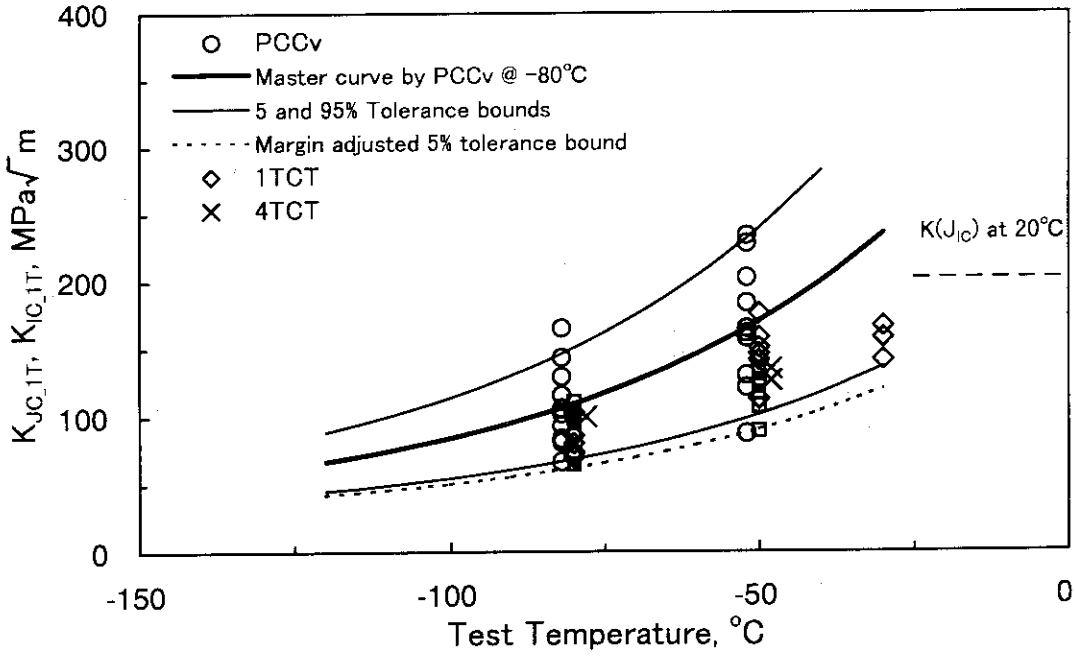

Figure 22--Size adjusted data to 1T, the master curve and torelance bound curves determined by PCCv data of Steel A.

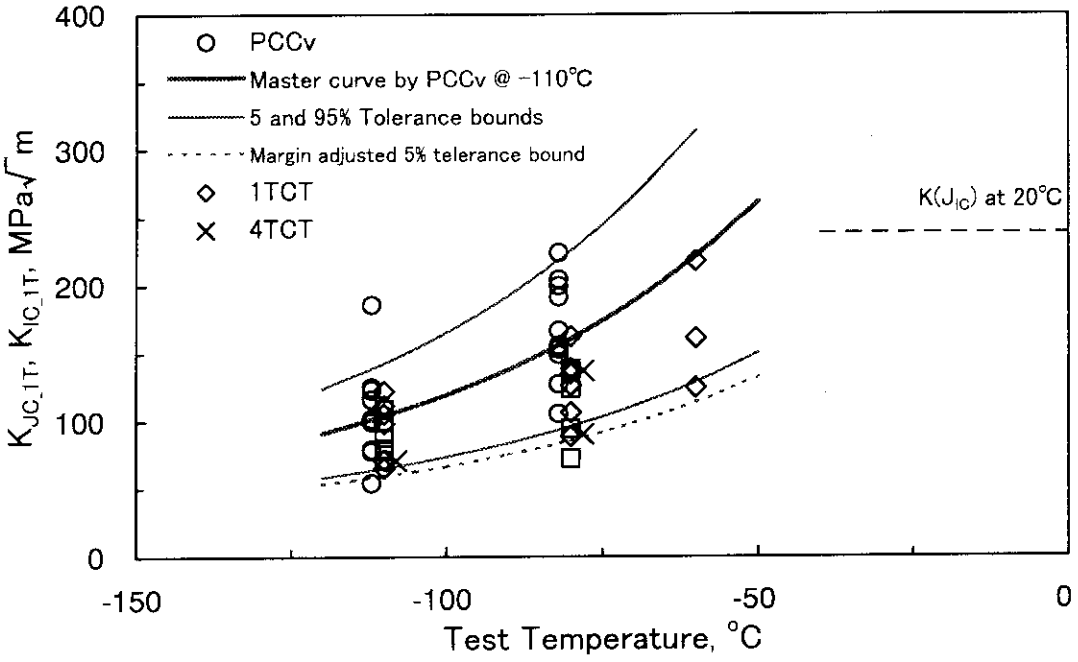

Figure 23--Size adjusted data to 1T, the master curve and tolerance bound curves determined by PCCv data of Steel B.

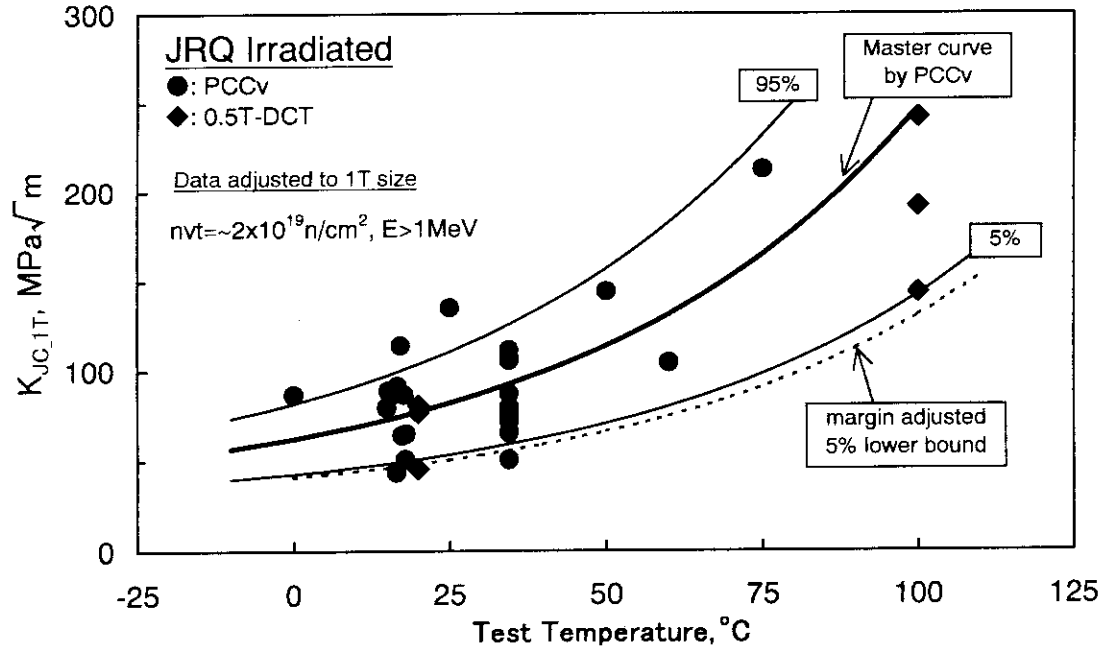

Figure 24--Size adjusted data to 1T, the master curve and tolerance bound curves determined by PCCv data of irradiated JRQ steel.

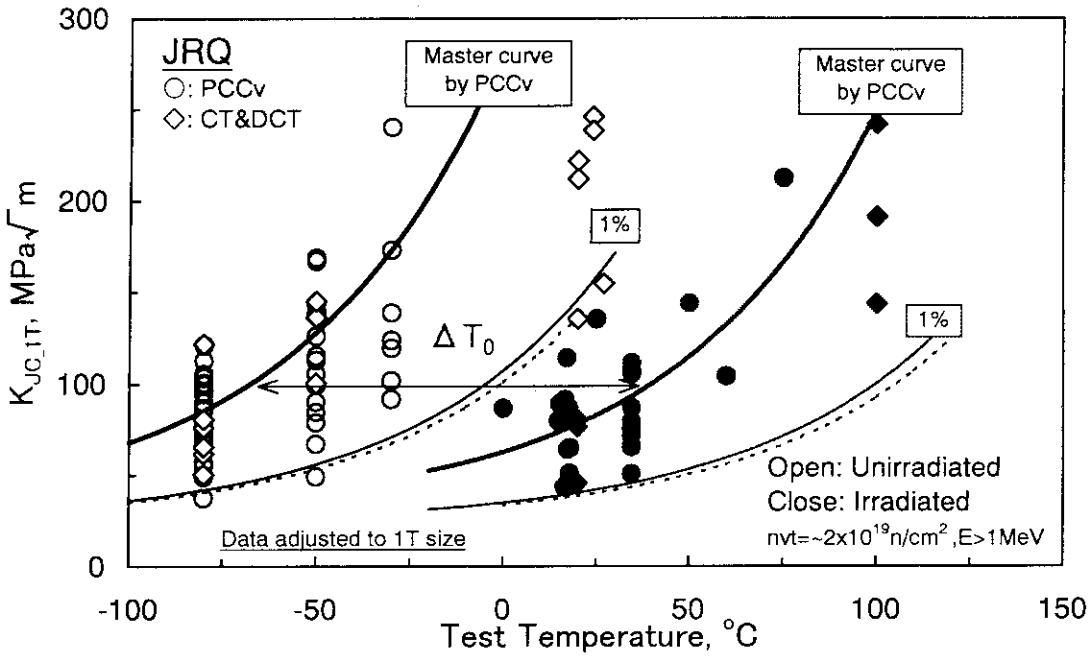

Figure 25--Effect of neutron irradiation on fracture toughness values adjusted to 1T and the master curve.

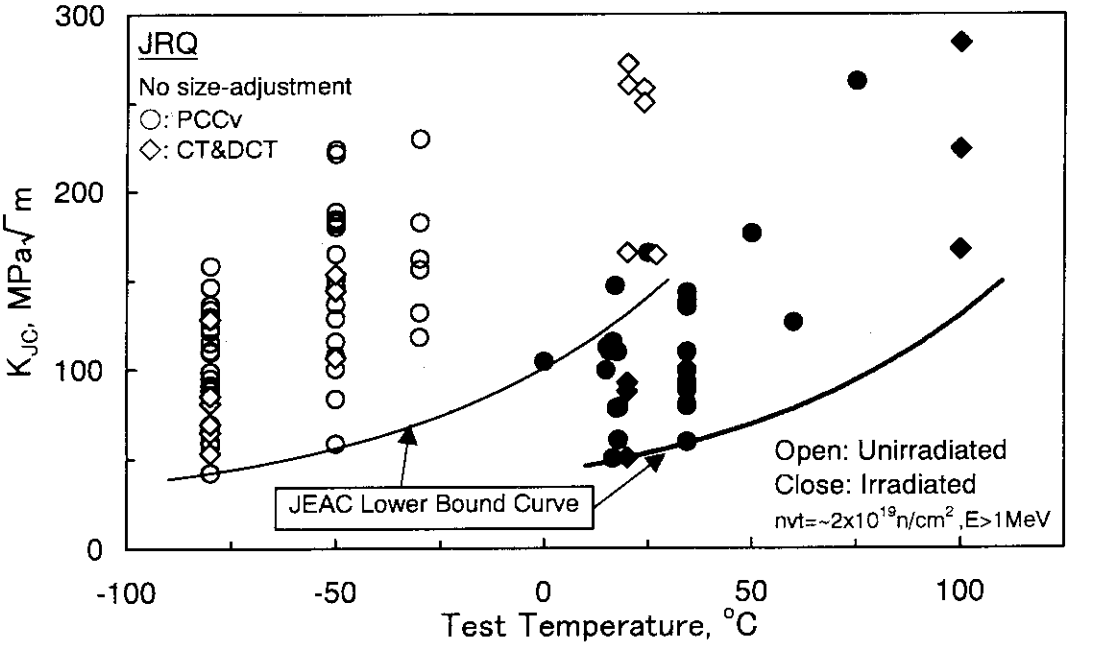

Figure 26--Lower bound curves according to the JEAC K_{IC} curve for JRQ steel before and after irradiation.

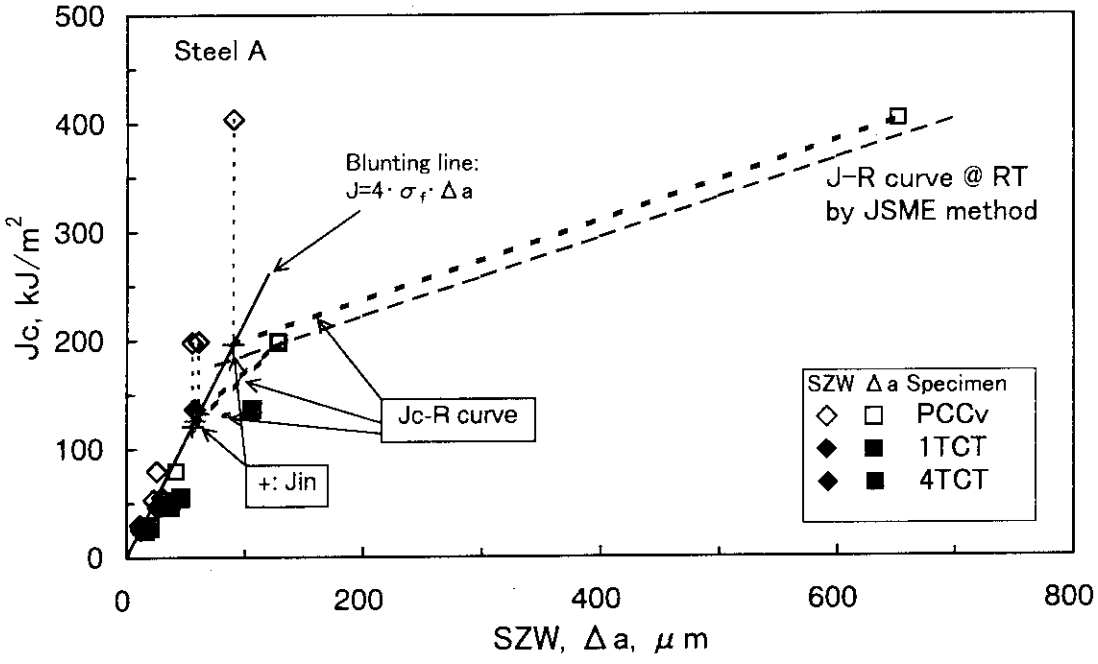

Figure 27--J-integral value at cleavage fracture versus ductile crack extension obtained from fractography of some specimens of Steel A.

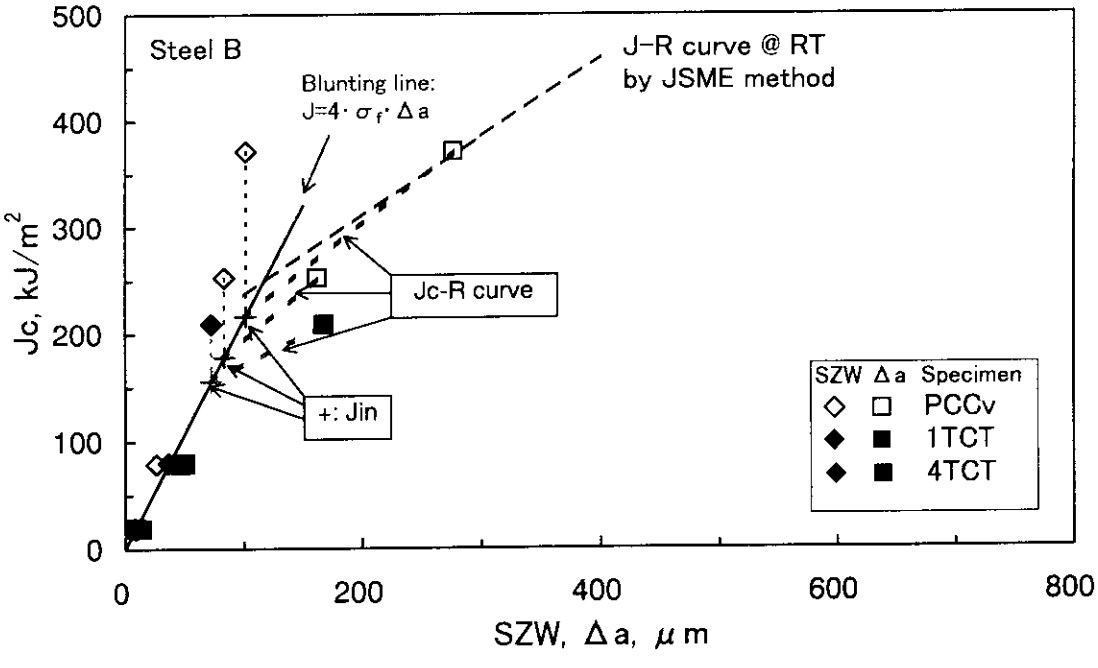

Figure 28--J-integral value at cleavage fracture versus ductile crack extension obtained from fractography of some specimens of Steel B.

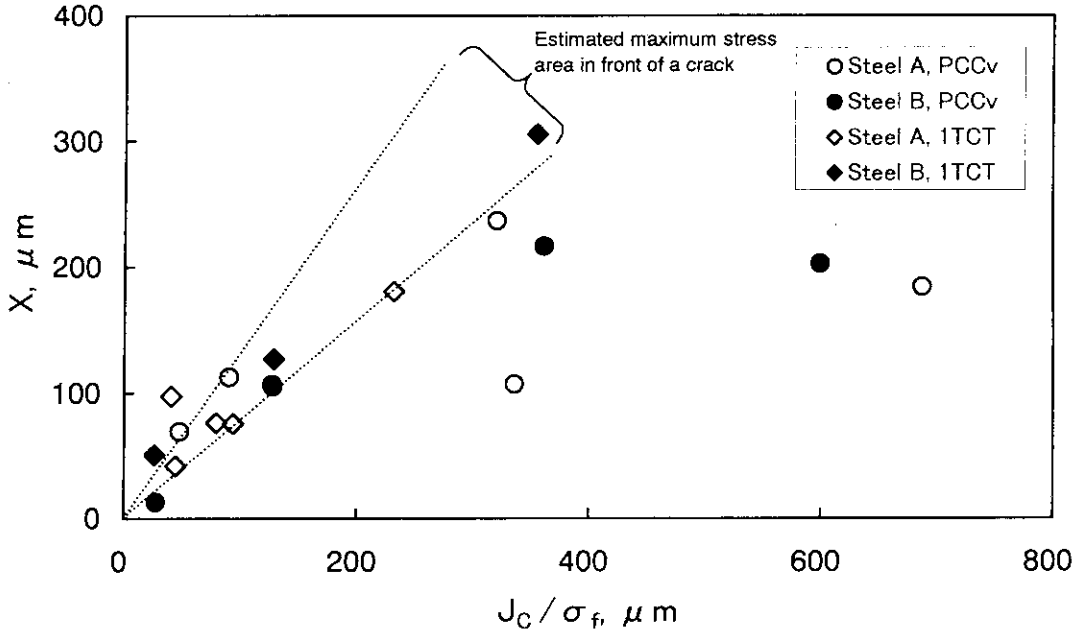

Figure 29--Distance from ductile crack front to cleavage initiation site as a function of J-integral.

APPENDIX

Table A-1 Fracture toughness test results of unirradiated JRQ.

TP ID.	Temp.	W	B	BN	a0	K_{Jc-89}	K_{JC-13}	K_{Jc_1T}	Specimen	Note
	℃	mm	mm	mm	mm	MPa√m	MPa√m	MPa√m		
Q26R	-80	10.0	10.0	10.0	5.49	88.4	83.8	70.7	PCCV	No SG
Q28R	-80	10.0	10.0	10.0	5.59	158.0	147.1	121.1	PCCV	No SG
Q29R	-80	10.0	10.0	10.0	5.55	121.5	113.9	94.6	PCCV	No SG
Q30R	-80	10.0	10.0	10.0	5.52	110.4	103.8	86.6	PCCV	No SG
Q31R	-80	10.0	10.0	10.0	5.25	122.9	115.2	95.7	PCCV	No SG
Q32R	-80	10.0	10.0	10.0	5.36	42.2	41.9	37.4	PCCV	No SG
Q33R	-80	10.0	10.0	10.0	5.23	109.7	103.0	86.0	PCCV	No SG
Q35R	-80	10.0	10.0	10.0	5.32	114.9	107.8	89.8	PCCV	No SG
Q36R	-80	10.0	10.0	10.0	5.31	85.4	81.1	68.6	PCCV	No SG
Q37R	-80	10.0	10.0	10.0	5.25	59.6	57.8	50.0	PCCV	No SG
Q38R	-80	10.0	10.0	10.0	5.22	115.1	108.0	90.0	PCCV	No SG
Q46R	-80	10.0	10.0	10.0	5.18	146.1	136.4	112.6	PCCV	No SG
Q50R	-80	10.0	10.0	10.0	5.17	133.5	124.9	103.4	PCCV	No SG
Q52R	-80	10.0	10.0	10.0	5.01	69.2	66.3	56.9	PCCV	No SG
Q53R	-80	10.0	10.0	10.0	5.08	57.9	56.5	49.0	PCCV	No SG
Q54R	-80	10.0	10.0	10.0	5.16	66.2	64.1	55.1	PCCV	No SG
Q73R	-80	10.0	10.0	8.0	5.58	91.0	86.2	72.6	PCCV	20% SG
Q74R	-80	10.0	10.0	8.0	5.64	136.1	127.3	105.3	PCCV	20% SG
Q75R	-80	10.0	10.0	8.0	5.61	98.6	93.0	78.1	PCCV	20% SG
Q76R	-80	10.0	10.0	8.0	5.78	128.1	119.9	99.4	PCCV	20% SG
Q77R	-80	10.0	10.0	8.0	5.54	129.6	121.3	100.6	PCCV	20% SG
Q78R	-80	10.0	10.0	8.0	5.60	94.8	89.7	75.4	PCCV	20% SG
Q80R	-80	10.0	10.0	8.0	5.64	98.4	92.9	78.0	PCCV	20% SG
RQ2	-80	10.0	10.0	7.9	5.60	90.7	86.0	72.5	PCCV	20% SG
Q40R	-50	10.0	10.0	10.0	5.16	83.3	79.2	67.1	PCCV	No SG
Q41R	-50	10.0	10.0	10.0	5.27	188.3	174.9	143.2	PCCV	No SG
Q42R	-50	10.0	10.0	10.0	5.31	115.5	108.3	90.2	PCCV	No SG
Q44R	-50	10.0	10.0	10.0	5.13	164.7	153.3	126.0	PCCV	No SG
Q45R	-50	10.0	10.0	10.0	5.29	107.7	101.3	84.6	PCCV	No SG
Q49R	-50	10.0	10.0	10.0	5.16	184.3	171.2	140.2	PCCV	No SG
Q51R	-50	10.0	10.0	10.0	5.11	128.3	120.0	99.5	PCCV	No SG
Q55R	-50	10.0	10.0	10.0	5.18	150.1	140.0	115.4	PCCV	No SG
Q56R	-50	10.0	10.0	10.0	5.06	180.0	167.3	137.1	PCCV	No SG
Q57R	-50	10.0	10.0	10.0	5.12	100.1	94.1	79.0	PCCV	No SG
Q61R	-50	10.0	10.0	10.0	5.42	58.4	56.7	49.2	PCCV	No SG
Q62R	-50	10.0	10.0	10.0	5.14	221.3	205.1	167.2	PCCV	No SG
Q65R	-50	10.0	10.0	10.0	5.22	136.5	127.4	105.4	PCCV	No SG
Q67R	-50	10.0	10.0	10.0	5.70	146.7	136.8	112.9	PCCV	No SG
Q68R	-50	10.0	10.0	10.0	5.93	182.4	169.3	138.8	PCCV	No SG
Q69R	-50	10.0	10.0	10.0	5.69	223.8	207.3	168.9	PCCV	No SG
Q39R	-30	10.0	10.0	10.0	5.28	~~321.7~~	~~297.1~~	~~240.4~~	PCCV	No SG
Q58R	-30	10.0	10.0	10.0	5.18	131.5	122.8	101.8	PCCV	No SG
Q60R	-30	10.0	10.0	10.0	5.10	155.8	145.0	119.4	PCCV	No SG
Q63R	-30	10.0	10.0	10.0	5.19	229.7	212.7	173.2	PCCV	No SG
Q64R	-30	10.0	10.0	10.0	5.25	161.9	150.6	123.8	PCCV	No SG
Q70R	-30	10.0	10.0	10.0	5.55	117.8	110.3	91.8	PCCV	No SG
Q72R	-30	10.0	10.0	10.0	5.67	182.3	169.3	138.7	PCCV	No SG
RQ4	-80	50.0	25.0	20.1	25.64	53.1	50.2	50.2	1TCT	20% SG
RQ10	-80	50.0	25.0	19.9	25.63	64.6	61.6	61.6	1TCT	20% SG
RQ6	-80	50.0	25.0	20.0	25.67	69.3	65.5	65.5	1TCT	20% SG
RQ3	-80	50.0	25.0	20.0	25.42	80.8	76.3	76.3	1TCT	20% SG
RQ2	-80	50.0	25.0	20.2	25.59	85.1	80.4	80.5	1TCT	20% SG
RQ9	-80	50.0	25.0	19.9	25.57	127.9	122.0	121.8	1TCT	20% SG
RQ5	-50	50.0	25.0	20.1	25.58	144.0	136.1	136.2	1TCT	20% SG
RQ7	-50	50.0	25.0	20.0	25.47	106.3	100.4	100.4	1TCT	20% SG
RQ8	-50	50.0	25.0	20.1	25.31	153.3	144.8	145.0	1TCT	20% SG
Q1CT	24	50.0	25.0	20.0	28.37	258.0	246.1	246.1	1TCT	20% SG
Q2CT	24	50.0	25.0	20.0	28.56	250.0	238.4	238.4	1TCT	20% SG
RQ1	27	50.0	25.0	20.0	25.22	163.9	154.8	154.8	1TCT	20% SG
Q31	20	25.0	12.5	10.0	15.18	272.0	259.9	221.8	0.5TDCT	20% SG
Q32	20	25.0	12.5	10.0	14.88	260.0	248.2	211.9	0.5TDCT	20% SG
Q33	20	25.0	12.5	10.0	15.11	165.0	157.2	135.4	0.5TDCT	20% SG
Q27	-75	10.0	10.0	10.0	5.71	66.9	63.9	56.9	PCCv	No SG
Q22	-50	10.0	10.0	10.0	5.75	259.7	247.8	211.4	PCCv	No SG
Q28	-40	10.0	10.0	10.0	5.71	161.0	153.6	132.3	PCCv	No SG
Q25	-25	10.0	10.0	10.0	5.87	207.6	198.0	169.6	PCCv	No SG

—: No cleavage fracture

Table A-2 Fracture toughness test results of irradiated JRQ.

TP ID.	Temp. ℃	W mm	B mm	BN mm	a0 mm	K_{Jc-89} MPavm	K_{Jc-13} MPavm	K_{Jc-13_1T} MPavm	Fluence n/cm^2	Specimen	Note
Q25R	16.5	10.0	10.0	10.0	5.39	50.0	49.6	43.5	1.8E+19	PCCv	No SG
Q20R	17.9	10.0	10.0	10.0	5.00	60.4	59.0	51.0	1.8E+19	PCCv	No SG
Q6R	17.4	10.0	10.0	10.0	5.16	78.6	76.6	65.0	2.6E+19	PCCv	No SG
Q4R	18.0	10.0	10.0	10.0	5.11	77.8	75.5	64.2	1.8E+19	PCCv	No SG
Q5R	14.9	10.0	10.0	10.0	5.15	99.2	95.0	79.7	2.3E+19	PCCv	No SG
Q13R	17.7	10.0	10.0	10.0	5.24	110.2	105.1	87.7	2.6E+19	PCCv	No SG
Q24R	16.8	10.0	10.0	10.0	5.35	110.0	104.7	87.4	1.6E+19	PCCv	No SG
Q19R	15.7	10.0	10.0	10.0	5.38	112.2	106.9	89.1	2.4E+19	PCCv	No SG
Q22R	15.2	10.0	10.0	10.0	5.01	109.4	103.8	86.7	1.9E+19	PCCv	No SG
Q3R	16.4	10.0	10.0	10.0	5.11	113.5	108.1	90.0	1.7E+19	PCCv	No SG
Q12R	16.6	10.0	10.0	10.0	5.24	115.2	109.7	91.3	2.3E+19	PCCv	No SG
Q11R	17.1	10.0	10.0	10.0	5.32	146.5	138.4	114.2	2.2E+19	PCCv	No SG
Q18R	34.5	10.0	10.0	10.0	5.36	59.3	58.5	50.6	2.2E+19	PCCv	No SG
Q15R	34.5	10.0	10.0	10.0	5.29	79.4	77.1	65.4	2.2E+19	PCCv	No SG
Q09R	34.5	10.0	10.0	10.0	5.26	80.0	77.8	66.0	2.2E+19	PCCv	No SG
Q14R	34.5	10.0	10.0	10.0	5.26	88.4	85.3	71.9	2.0E+19	PCCv	No SG
Q1R	34.5	10.0	10.0	10.0	5.33	92.8	89.1	75.0	2.0E+19	PCCv	No SG
Q10R	34.5	10.0	10.0	10.0	5.32	99.1	94.9	79.5	2.0E+19	PCCv	No SG
Q02R	34.5	10.0	10.0	10.0	5.34	109.5	104.3	87.0	2.2E+19	PCCv	No SG
Q21R	34.5	10.0	10.0	10.0	5.36	134.8	127.5	105.5	2.0E+19	PCCv	No SG
Q08R	34.5	10.0	10.0	10.0	5.32	137.4	130.0	107.5	2.0E+19	PCCv	No SG
Q23R	34.5	10.0	10.0	10.0	5.35	143.0	135.0	111.5	2.1E+19	PCCv	No SG

TP ID.	Temp. ℃	W mm	B mm	BN mm	a0 mm	K_{Jc-89} MPavm	K_{Jc-13} MPavm	K_{Jc-13_1T} MPavm	Fluence n/cm^2	Specimen	Note
Q8	0	10.0	10.0	10.0	5.39	102.9	98.2	85.7	2.3E+19	PCCv	No SG, Ref(11)
Q9	25	10.0	10.0	10.0	5.57	164.3	156.7	134.8	2.0E+19	PCCv	No SG, Ref(11)
Q10	50	10.0	10.0	10.0	5.57	175.8	167.7	144.1	2.3E+19	PCCv	No SG, Ref(11)
Q14	60	10.0	10.0	10.0	5.54	125.6	119.8	103.9	2.3E+19	PCCv	No SG, Ref(11)
Q11	75	10.0	10.0	10.0	5.45	262.2	250.1	213.4	2.0E+19	PCCv	No SG, Ref(11)
Q1	20	25.0	12.5	10.0	13.68	87.4	87.4	80.0	2.3E+19	0.5TDCT	20% SG, Ref(11)
Q18	20	25.0	12.5	10.0	13.56	50.4	50.4	47.0	2.4E+19	0.5TDCT	20% SG, Ref(11)
Q19	20	25.0	12.5	10.0	13.53	92.1	92.1	84.1	2.3E+19	0.5TDCT	20% SG, Ref(11)
Q3	100	25.0	12.5	10.0	13.68	291.2	277.8	249.3	2.4E+19	0.5TDCT	20% SG, Ref(11)
Q6	100	25.0	12.5	10.0	13.62	230.1	219.5	197.5	2.5E+19	0.5TDCT	20% SG, Ref(11)
Q17	100	25.0	12.5	10.1	13.73	170.6	162.8	147.0	2.5E+19	0.5TDCT	20% SG, Ref(11)
Q21	20	25.0	12.5	10.0	13.67	63.7	63.7	58.9	4.6E+19	0.5TDCT	20% SG, Ref(11)
Q22	20	25.0	12.5	10.0	13.50	55.2	55.2	51.3	4.5E+19	0.5TDCT	20% SG, Ref(11)
Q23	100	24.9	12.5	10.0	13.71	98.9	98.9	90.2	4.5E+19	0.5TDCT	20% SG, Ref(11)
Q24	100	25.0	12.5	10.0	13.58	85.4	85.4	78.2	4.5E+19	0.5TDCT	20% SG, Ref(11)

Table A-3 Fracture toughness test results of steel A.

TP ID	Temp. ℃	W mm	B mm	BN mm	a0 mm	K_{JC-89} MPa$\sqrt{m}$	K_{JC_13} MPa$\sqrt{m}$	K_{Jc_1T} MPa$\sqrt{m}$	Specimen
AP115	-80	10.01	10.01	7.97	5.09	81.3	78.3	66.4	PCCv
AP122	-80	10.01	10.01	8.00	5.12	101.5	96.6	81.0	PCCv
AP123	-80	10.01	10.02	7.99	5.10	104.7	99.5	83.3	PCCv
AP124	-80	10.01	10.01	8.04	5.18	118.2	112.0	93.2	PCCv
AP121	-80	10.02	10.01	8.09	5.08	130.0	122.6	101.7	PCCv
AP119	-80	10.01	10.01	8.02	5.21	135.2	127.7	105.7	PCCv
AP114	-80	10.02	10.02	8.06	5.15	148.2	139.6	115.1	PCCv
AP120	-80	10.01	10.01	7.98	5.25	166.8	156.9	128.9	PCCv
AP125	-80	10.01	10.01	8.01	5.13	186.1	174.7	143.0	PCCv
AP116	-80	10.01	10.01	8.02	5.14	215.9	202.3	165.0	PCCv
AP104	-50	10.01	10.01	8.01	5.24	110.4	104.4	87.2	PCCv
AP112	-50	10.01	10.01	8.03	5.20	156.3	146.9	120.9	PCCv
AP113	-50	10.01	10.01	8.04	5.28	168.5	158.1	129.9	PCCv
AP103	-50	10.01	10.02	8.10	5.11	205.9	192.7	157.4	PCCv
AP111	-50	10.01	10.01	7.96	5.23	211.0	197.6	161.3	PCCv
AP110	-50	10.01	10.01	8.04	5.15	215.6	201.8	164.7	PCCv
AP108	-50	10.02	10.02	8.03	5.11	241.3	225.5	183.5	PCCv
AP107	-50	10.02	10.02	7.98	5.38	266.8	249.2	202.4	PCCv
AP106	-50	10.02	10.02	8.05	5.16	301.4	281.0	227.7	PCCv
AP109	-50	10.01	10.01	8.00	5.23	309.3	288.4	233.5	PCCv

TP ID	Temp. ℃	W mm	B mm	BN mm	a0 mm	K_{Jc} MPa$\sqrt{m}$	K_{Jc_13} MPa$\sqrt{m}$	Specimen
AK103	-80	50.04	25.02	20.02	29.64	64.3	64.2	1TCT
AK2	-80	49.99	25.00	20.00	28.59	70.1	69.9	1TCT
AK6	-80	50.01	25.00	20.01	28.57	72.9	72.6	1TCT
AK4	-80	50.00	24.99	20.04	28.73	73.8	73.5	1TCT
AK1	-80	50.00	25.00	19.99	28.55	80.0	79.6	1TCT
AK5	-80	50.00	25.00	20.01	28.77	85.6	85.2	1TCT
AK105	-80	50.00	25.02	20.00	29.08	87.8	87.5	1TCT
AK104	-80	50.02	25.00	20.02	29.30	94.9	94.4	1TCT
AK101	-80	50.02	25.02	20.00	29.24	97.5	97.0	1TCT
AK102	-80	50.02	25.02	20.00	29.05	99.9	99.3	1TCT
AK3	-80	50.00	24.99	20.03	28.55	103.1	102.2	1TCT
AK106	-80	50.02	25.00	20.02	29.32	110.4	109.6	1TCT
AK107	-50	50.02	25.02	20.02	29.21	89.0	88.5	1TCT
AK109	-50	50.04	25.02	20.00	29.54	107.1	106.3	1TCT
AK9	-50	49.99	25.00	19.99	28.59	112.5	111.0	1TCT
AK111	-50	50.02	25.00	20.02	29.06	117.2	116.0	1TCT
AK110	-50	50.00	25.02	20.02	29.22	121.5	120.3	1TCT
AK112	-50	50.02	25.00	20.02	29.37	132.4	130.6	1TCT
AK108	-50	50.04	25.02	20.02	29.01	135.0	133.2	1TCT
AK11	-50	49.99	25.00	20.01	28.54	141.0	138.4	1TCT
AK7	-50	50.00	25.00	20.01	29.10	145.8	142.8	1TCT
AK12	-50	50.00	25.00	20.05	28.46	150.7	147.4	1TCT
AK8	-50	50.01	24.99	20.02	28.71	158.2	154.5	1TCT
AK10	-50	50.00	25.00	20.03	28.64	175.7	170.9	1TCT
AK14	-30	49.97	24.99	20.00	28.83	141.5	138.7	1TCT
AK15	-30	49.98	25.00	19.98	28.90	157.8	153.9	1TCT
AK13	-30	49.98	25.00	20.00	29.03	166.3	162.2	1TCT

TP ID	Temp. ℃	W mm	B mm	a0 mm	K_Q MPa$\sqrt{m}$	K_{Q_1T} MPa$\sqrt{m}$	Validity for K_{IC}	Specimen
AK1	-80	200.3	106.2	101.2	75.8	99.1	○	4TCT
AK2	-50	200.4	106.6	101.4	102.8	137.5	×	4TCT
AK3	-50	200.5	105.6	100.0	96.7	128.4	○	4TCT

Table A-4 Fracture toughness test results of steel B.

TP ID	Temp. ℃	W mm	B mm	BN mm	a0 mm	K_{JC-89} MPa$\sqrt{m}$	K_{JC_13} MPa$\sqrt{m}$	K_{Jc_1T} MPa$\sqrt{m}$	Specimen
BP119	-110	10.01	10.02	8.04	5.01	64.7	63.2	54.4	PCCv
BP124	-110	10.02	10.01	8.05	5.12	97.0	92.7	77.9	PCCv
BP120	-110	10.01	10.01	7.99	5.14	97.6	93.1	78.2	PCCv
BP127	-110	10.02	10.01	8.03	5.23	98.9	94.2	79.1	PCCv
BP123	-110	10.02	10.02	8.03	5.13	126.5	119.9	99.5	PCCv
BP121	-110	10.01	10.02	8.05	5.18	129.6	122.6	101.6	PCCv
BP126	-110	10.01	10.01	8.04	5.07	149.3	140.8	116.1	PCCv
BP117	-110	10.01	10.02	8.03	5.08	158.6	149.4	122.9	PCCv
BP118	-110	10.02	10.01	8.02	5.25	161.5	152.0	125.0	PCCv
BP115	-110	10.02	10.02	8.03	5.30	243.8	228.3	185.7	PCCv
BP108	-80	10.01	10.01	8.03	5.31	135.1	127.5	105.5	PCCv
BP102	-80	10.01	9.98	8.08	5.13	165.0	155.1	127.4	PCCv
BP104	-80	10.02	10.01	8.05	5.01	194.3	182.4	149.1	PCCv
BP103	-80	10.02	9.99	8.08	5.15	200.4	187.8	153.4	PCCv
BP112	-80	10.02	10.02	8.03	5.07	203.4	190.7	155.8	PCCv
BP114	-80	10.02	10.02	8.05	5.01	218.0	204.2	166.6	PCCv
BP113	-80	10.01	10.01	8.06	5.01	252.0	235.7	191.6	PCCv
BP111	-80	10.02	10.02	7.98	5.19	263.0	245.8	199.7	PCCv
BP109	-80	10.01	10.02	8.00	5.27	269.7	252.0	204.6	PCCv
BP101	-80	10.02	10.02	8.03	5.12	296.0	276.6	224.2	PCCv

TP ID	Temp. ℃	W mm	B mm	BN mm	a0 mm	K_{Jc} MPa$\sqrt{m}$	K_{Jc_13} MPa$\sqrt{m}$	Specimen
BK5	-110	50.02	25.00	19.99	28.89	65.4	65.2	1TCT
BK101	-110	50.02	25.04	20.00	29.12	71.2	71.1	1TCT
BK3	-110	50.02	25.00	19.99	28.67	71.3	71.0	1TCT
BK104	-110	50.02	25.02	20.02	29.17	78.3	78.1	1TCT
BK106	-110	50.02	25.02	20.00	29.73	79.9	79.6	1TCT
BK103	-110	50.00	25.02	20.02	28.96	87.9	87.6	1TCT
BK6	-110	50.01	25.00	20.00	28.63	98.5	97.7	1TCT
BK102	-110	50.00	25.04	20.02	28.98	99.8	99.3	1TCT
BK2	-110	50.00	24.99	19.99	29.38	105.5	104.3	1TCT
BK105	-110	50.02	25.02	20.02	29.31	108.7	108.0	1TCT
BK4	-110	50.04	25.00	20.00	29.27	111.6	110.5	1TCT
BK1	-110	50.03	25.00	20.03	28.79	122.0	120.8	1TCT
BK112	-80	50.02	25.02	20.00	29.06	72.4	72.3	1TCT
BK11	-80	50.01	25.00	20.00	28.81	88.9	88.4	1TCT
BK111	-80	50.02	25.02	20.00	29.22	94.7	94.2	1TCT
BK10	-80	50.01	25.00	20.01	29.22	106.6	105.4	1TCT
BK110	-80	50.00	25.02	20.00	29.35	124.2	122.8	1TCT
BK12	-80	50.00	25.00	20.00	28.54	126.4	124.6	1TCT
BK8	-80	50.02	24.99	20.00	28.74	135.2	132.8	1TCT
BK109	-80	50.00	25.02	20.02	29.48	135.7	134.1	1TCT
BK107	-80	50.02	25.02	20.02	29.08	136.9	135.2	1TCT
BK108	-80	50.02	25.04	20.02	29.40	138.7	136.9	1TCT
BK7	-80	50.02	25.00	20.02	28.88	139.0	136.4	1TCT
BK9	-80	50.00	25.00	20.04	28.43	162.5	158.6	1TCT
BK13	-60	50.00	25.00	20.05	28.80	124.7	122.8	1TCT
BK15	-60	50.02	25.00	20.01	28.89	161.2	157.4	1TCT
BK14	-60	50.02	25.00	20.03	29.19	218.1	211.0	1TCT

TP ID	Temp. ℃	W mm	B mm	a0 mm	K_Q MPa$\sqrt{m}$	K_{Q_1T} MPa$\sqrt{m}$	Validity for K_{IC}	Specimen
BK1	-110	200.4	106.4	101.5	55.9	71.0	○	4TCT
BK2	-80	200.2	108.9	101.5	69.6	90.5	○	4TCT
BK3	-80	200.2	107.0	101.3	102.6	137.2	○	4TCT